Early Colony Establishment in *Neurospora crassa* Requires a MAP Kinase Regulatory Network

Abigail C. Leeder,[1] Wilfried Jonkers,[1] Jingyi Li,[2] and N. Louise Glass[3]
Department of Plant and Microbial Biology, University of California, Berkeley, California 94720-3102

ABSTRACT Vegetative fusion is essential for the development of an interconnected colony in many filamentous fungi. In the ascomycete fungus *Neurospora crassa*, vegetative fusion occurs between germinated conidia (germlings) via specialized structures termed "conidial anastomosis tubes" (CATs) and between hyphae within a mature colony. In *N. crassa*, both CAT and hyphal fusion are under the regulation of a conserved MAP kinase cascade (NRC1, MEK2, and MAK2). Here we show that the predicted downstream target of the MAK2 kinase pathway, a Ste12-like transcription factor known as PP1, regulates elements required for CAT and hyphal fusion. The PP1 regulatory network was revealed by expression profiling of wild type and the Δ*pp-1* mutant during conidial germination and colony establishment. To identify targets required for cell fusion more specifically, expression-profiling differences were assessed via inhibition of MAK2 kinase activity during chemotropic interactions and cell fusion. These approaches led to the identification of new targets of the cell fusion pathway that, when mutated, showed alterations in chemotropic signaling and cell fusion. In particular, conidial germlings carrying a deletion of NCU04732 (Δ*ham-11*) failed to show chemotropic interactions and cell fusion. However, signaling (as shown by oscillation of MAK2 and SO to CAT tips), chemotropism, and cell fusion were restored in Δ*ham-11* germlings when matched with wild-type partner germlings. These data reveal novel insights into the complex process of self-signaling, germling fusion, and colony establishment in filamentous fungi.

CELL fusion between genetically identical cells is important in development (for example, myoblast fusion during muscle formation) and occurs in many multicellular organisms from simple ascomycete fungi to mammals (Chen *et al.* 2007; Aguilar *et al.* 2013). Cell fusion between genetically identical cells can be mediated by cells that have differentiated, but in some cases, also between cells in an identical developmental state, for example, cell fusion between germinating asexual spores (conidia) of filamentous fungi (Pandey *et al.* 2004; Roca *et al.* 2005a; Read *et al.* 2010). In filamentous fungi, these fusions are integral to the formation of an interconnected hyphal network, which mediates genetic mixing and the sharing of resources (Simonin *et al.* 2012; Roper *et al.* 2013). How this process is initiated and maintained and what proteins are involved are still mostly unknown.

doi: 10.1534/genetics.113.156984
Manuscript received July 1, 2013; accepted for publication September 4, 2013
Supporting information is available online at http://www.genetics.org/lookup/suppl/doi:10.1534/genetics.113.156984/-/DC1.
[1]These authors contributed equally to this work.
[2]Present address: Genomatica Inc., 10520 Wateridge Circle, San Diego, CA 92121.
[3]Corresponding author: University of California, 111 Koshland Hall, #3102, Berkeley, CA 94720-3102. E-mail: lglass@berkeley.edu

In filamentous ascomycete fungi, a conserved MAP kinase pathway that is involved in pheromone response and mating in *Saccharomyces cerevisiae* (Ste11, Ste7, and Fus3) (Bardwell 2005) is required for cell fusion and heterokaryon formation during vegetative growth (Hou *et al.* 2002; Wei *et al.* 2003; Pandey *et al.* 2004; Fu *et al.* 2011; Jun *et al.* 2011; Dettmann *et al.* 2012). This conserved pathway also plays a role in sexual development and secondary metabolism and is required for the virulence of both plant and animal fungal pathogens (Roman *et al.* 2007; Rispail and Di Pietro 2010; Bayram *et al.* 2012). In *S. cerevisiae*, reception of a mating-type-specific pheromone signal results in the activation of Ste11 (MEKK), Ste7 (MEK), and Fus3 (MAPK) (Bardwell 2005). After Fus3 is activated, it enters the nucleus and phosphorylates Ste12, a mating-type-specific transcription factor, as well as two regulators of Ste12, Dig1 and Dig2 (Blackwell *et al.* 2007). Activated Ste12 regulates the expression of many genes involved in the mating process, both indirectly and directly by binding pheromone response elements in target promoters (Zeitlinger *et al.* 2003).

Ste12-like proteins have also been studied in filamentous fungi, where they play essential roles in development and

pathogenicity (Alspaugh *et al.* 1998; Vallim *et al.* 2000; Borneman *et al.* 2001; Park *et al.* 2002; Tsuji *et al.* 2003; Li *et al.* 2005; Nolting and Poggeler 2006; Ren *et al.* 2006; Tollot *et al.* 2009; Rispail and Di Pietro 2010; Wong Sak Hoi and Dumas 2010). Fus3-like proteins in filamentous fungi could directly or indirectly phosphorylate Ste12-like proteins, but this has not yet been shown in any system. However, strains carrying deletions of Fus3-like proteins or Ste12-like proteins often show a similar phenotype in many filamentous fungi, suggesting that Fus3-like kinases positively activate Ste12-like proteins. All Ste12-like proteins contain a divergent homeodomain (STE) near their N terminus, which is involved in DNA binding (Errede and Ammerer 1989). Ste12-like proteins in filamentous fungi also contain two C-terminal C2H2-Zn^{2+} motifs (Vallim *et al.* 2000; Chang *et al.* 2004) (Figure 1A) that are absent in *S. cerevisiae* and other related ascomycete yeast species. In the plant pathogen *Magnaporthe grisea*, both the STE domain and the C2H2-Zn^{2+} motifs of the *STE12* homolog, *mst12*, are essential for the development of appressorial penetration pegs (Park *et al.* 2004), while in the human basidiomycete pathogen *Cryptococcus neoformans*, the STE domain and the C2H2-Zn^{2+} motifs were important for function, although mutagenesis of each domain resulted in strains with different phenotypes (Chang *et al.* 2004). In *S. cerevisiae*, Ste12-binding partners include Mcm1 and Tec1 (Primig *et al.* 1991; Madhani and Fink 1997). In *Sordaria macrospora*, a physical interaction between STE12 and MCM1 is required for sexual spore formation (Nolting and Poggeler 2006).

In *Neurospora crassa*, proteins orthologous to the Fus3 MAP kinase pathway (NRC1, MEK2, MAK2) regulate vegetative cell fusion (Pandey *et al.* 2004; Fleissner *et al.* 2008; Fu *et al.* 2011; Dettmann *et al.* 2012). Cell fusion events are particularly frequent in germinating asexual spores (conidia) and are associated with the production of specialized fusion structures termed "conidial anastomosis tubes" (CATs) (Roca *et al.* 2005b). Chemotropic interactions occur when two neighboring germlings sense each other and redirect the growth of CATs. During chemotropic interactions, NRC1, MEK2, and MAK2 oscillate together from CAT tip to cytoplasm. The oscillation of NRC1/MEK2/MAK2 occurs every 4 min and is perfectly out of phase with a second protein, SO, which also oscillates from CAT tip to cytoplasm in communicating germling pairs (Fleissner *et al.* 2009b; Dettmann *et al.* 2012). A *STE12* homolog has also been identified in *N. crassa* (*pp-1*). A Δ*pp-1* mutant shows slow growth, is female sterile (they do not develop protoperithecia), and displays ascospore lethality (Li *et al.* 2005), phenotypes that are very similar to that displayed by Δ*mak-2* mutants. Previous analyses using a *N. crassa* partial-genome (13%) microarray identified genes whose expression is altered in a mature colony (7 days old) in the absence of *mak-2* or *pp-1*. These analyses revealed that PP1 is involved in the regulation of sexual development, asexual development, and secondary metabolism (Li *et al.* 2005).

In this study, we evaluated the role of PP1 during cell fusion of asexual spores and expanded analyses using whole-genome arrays and RNA-seq to examine the function of MAK2 and PP1 during germling fusion and early colony establishment. These analyses revealed MAK2- and PP1-dependent gene networks involved in various aspects of colony development and identified novel genes with important roles in regulating communication and chemotropic attraction between *N. crassa* germlings.

Materials and Methods

Molecular techniques and strain construction

All strains constructed and used in this study are listed in Table 1 and Table 2. Strains were grown on Vogel's minimal medium (VMM) (Vogel 1956) (with supplements as required) and were crossed on Westergaard's medium (Westergaard and Mitchell 1947). Transformations and other *N. crassa* molecular techniques were performed as described (Colot *et al.* 2006) or using protocols available at the *Neurospora* home page at the Fungal Genetics Stock Center (FGSC) (http://www.fgsc.net/neurospora/neurosporaprotocolguide.htm).

To construct the *pp-1* site-directed mutant alleles, fusion PCR was performed with the mutation included in the overlapping primer region (Supporting Information, Table S1). Alleles were cloned into *his-3* targeting plasmid pMF272 (AY598428) (Margolin *et al.* 1997; Freitag *et al.* 2004) and integrated into the *his-3* locus of a *his-3*; Δ*pp-1* strain. Δ*pp-1* and Δ*pp-1* transformant strains showing an ascospore lethal phenotype were mated to the *Diploid* (*Dip*) mutant strain (FGSC 9537) as described in Hutchison *et al.* (2009) to construct homokaryotic strains or strains containing auxotrophic markers. In *Dip* crosses, ~2/3 of the ascospores are large and diploid. Streaking *Dip* progeny onto sorbose plates results in restoration of haploid strains. The *pp-1* sequence in all engineered strains was confirmed by DNA sequence analyses.

Deletion strains were obtained from the FGSC (McCluskey 2003) and were generated as part of the *N. crassa* functional genomics project (Colot *et al.* 2006; Dunlap *et al.* 2007). For each deletion strain, both the mating type *A* and mating type *a* strains were analyzed, if available. The phenotypes of deletion strains that were available only as a single mating type from the FGSC (McCluskey 2003) were confirmed by segregation analysis. Ascospore progeny were selected from crosses with FGSC 2489 (mating type *A*) or FGSC 988 (mating type *a*) and assessed for phenotype and hygromycin resistance. To pass this test, hygromycin resistance had to segregate with fusion phenotype. In cases where deletion strains were not publicly available (genes with locus identification numbers: NCU00811, NCU00995, NCU01380, and NCU09693), we constructed deletion mutants using a *mus-51* background as described (Colot *et al.* 2006). Primers (Table S1) were designed to amplify

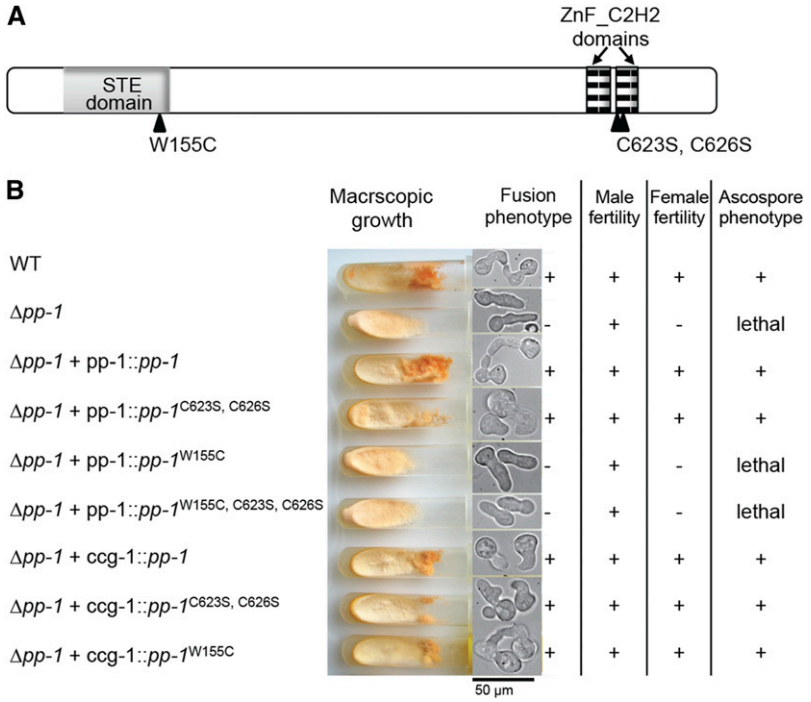

Figure 1 The homeodomain of PP1 is required for function. (A) Schematic representation of PP1 with protein domains depicted. Point mutations resulting in amino acid substitutions in the respective protein domains are indicated. (B) Phenotypic results of introduction of wild-type and mutated *pp-1* alleles into a Δ*pp-1* mutant. Strains with alleles are listed on the left, and phenotypic analyses are depicted or listed on the right.

the upstream and downstream flanks of these four genes, as well as the hygromycin cassette from plasmid pCSN44 (Colot *et al.* 2006). The two flanks, the hygromycin cassette and digested plasmid pRS426 (*Eco*RI and *Xho*I), were transformed into yeast, and recombined plasmids were obtained via plasmid rescue (Colot *et al.* 2006). Hygromycin transformants were crossed to wild type (WT) (FGSC 2489) to eliminate the *mus-51* mutation and to obtain homokaryotic progeny. The genotype of all deletion strains was confirmed by PCR, using a primer for the hygromycin cassette (HygRupflank) paired with a gene-specific primer from the flank region, as well as a gene-specific primer outside the gene and a gene-specific primer within the open reading frame (Table S1).

To construct the internally GFP-tagged *ham-11* construct, we amplified *ham-11* using primers 04732F and 04732R (Table S1) and cloned it into a pCR-Blunt vector (Invitrogen). We sequenced and digested the amplicon from the vector with *Bgl*II and *Apa*I. The *tef1* promoter was removed from plasmid *ptef1-mek-2-gfp* (Dettmann *et al.* 2012) with *Not*I and *Bam*HI. Using a three-point ligation, we cloned the *tef1* promoter and *ham-11* amplicon into plasmid pmf272 (Freitag *et al.* 2004), using *Not*I and *Apa*I. GFP containing codons for eight glycine linkers and a *Bam*HI restriction site on both ends was amplified from plasmid pMF272 using primers Fgfp+8xgly and Rgfp+8xgly (Table S1) and cloned into a pCR-Blunt vector (Invitrogen). We sequenced the amplicon, digested it with *Bam*HI, and ligated it into the *Bam*HI site in *ham-11* situated between the two predicted transmembrane domains. This *ham-11* construct with internally tagged *gfp* was transformed into the Δ*ham-11 his3*$^-$ strain with selection for His prototrophy. A homokaryotic strain was obtained via microconidia purification (Pandit and Maheshwari 1994).

Phenotypic analyses

Macroscopic growth differences were assessed by growing the different strains (WT, Δ*ham-7*, Δ*ham-11*, and Δ*ham-12*) in flasks for 1 week at 25° and on VMM plates for 2 days at 25°. Growth rate on VMM plates was measured at 25° by putting 1×10^6 conidia in the center of the plates and measuring the radial growth front after 24 and 48 hr. Aerial hyphae extension was determined by inoculating tubes containing 1 ml of liquid VMM with 1×10^6 conidia; aerial hyphae height was measured after 3 days of growth at 25° in constant light. Ten replicates were measured for each strain.

To assess the frequency of communication and fusion between conidia within a deletion strain as compared to wild type, slant tubes containing the strains were grown for 4–6 days or until significant conidiation occurred. Conidia were harvested by vortexing the slant tube with 2 ml ddH_2O and subsequently filtered by pouring over cheesecloth to remove hyphal fragments. Conidia were diluted to a concentration of 3.3×10^7 conidia/ml. For each sample, 300 µl of spore suspension was spread on a 9-cm solid VMM plate. The plates were dried in open air for 20–30 min and incubated for 3–4 hr at 30°. Squares of 1 cm were excised and observed with a Zeiss Axioskop 2 using a ×40 Plan-Neofluor oil immersion objective. For each strain, 50–100 germling pairs were counted in triplicate. The ability to communicate is given as a percentage of pairs that display homing behavior when germinated conidia are within ~15 µm of each other. To assess the frequency of communication between

Table 1 N. *crassa* strains used in this study

Name	Mutant genotype	Source
R13-5	Δ*pp-1 A*	Li *et al.* (2005)
	Δ*pp-1 a*	This study
FGSC 9537	*Dip*	FGSC
FGSC 6103	*his-3 A*	FGSC
	his-3; Δ*pp-1 A*	This study
	his-3^{+}::*Pccg1 pp-1*^{W155C} *a*	This study
	his-3^{+}::*pp-1*^{W155C} *a*	This study
	his-3^{+}::*pp-1*$^{W155C,\ C623S,\ C626S}$ *a*	This study
	his-3^{+}::*Pccg1 pp-1*$^{C623S,\ C626S}$ *a*	This study
	his-3^{+}::*pp-1*$^{C623S,\ C626S}$ *a*	This study
	his-3^{+}::*Pccg1 pp-1 a*	This study
	his-3^{+}::*pp-1 a*	This study
mal1	*his-3*$^{+}$::*Pccg1 mak-2*^{Q100G}; Δ*mak-2 A*	Fleissner *et al.* (2009b)
FGSC 9718	Δ*mus-51*::*bar a*	FGSC
FGSC 988	Oak Ridge WT *a*	FGSC
FGSC 2489	Oak Ridge WT *A*	FGSC
R9-08	*hex-1 A*	Jedd and Chua (2000)
AF-SoT8	*his-3*$^{+}$::*Pccg1 so-gfp A*	Fleissner *et al.* (2009b)
AF-M512	*his-3*$^{+}$::*Pccg1 mak-2-gfp A*	Fleissner *et al.* (2009b)
	his-3; Δ*ham-7 A*	This study
	his-3^{+}::*Pccg1 so-gfp*; Δ*ham-7 A*	This study
	his-3^{+}::*Pccg1 mak-2-gfp*; Δ*ham-7 A*	This study
	his-3; Δ*ham-11 A*	This study
	his-3^{+}::*Pccg1 so-gfp*; Δ*ham-11 A*	This study
	his-3^{+}::*Pccg1 mak-2-gfp*; Δ*ham-11 A*	This study
	his-3^{+}::*Ptef1 ham-11-gfp*; Δ*ham-11 A*	This study
	his-3^{+}::*Pccg-1 Prm-1-gfp*; Δ*Prm-1 A*	Fleissner *et al.* (2009a)

conidia of a deletion strain with wild-type germlings, mixtures of *mak-2-gfp*- or *so-gfp*-expressing strains and non-fluorescing strains were prepared and similarly treated as described above.

Fluorescence microscopy

Molecular techniques, including SO-GFP and MAK2-GFP strain construction, were previously described (Fleissner *et al.* 2009b). The strain used to cross *so-gfp* into deletion strains was AF-SoT8, and the strain used to cross *mak-2-gfp* into deletion strains was AF-M512 (Table 1) (Fleissner *et al.* 2009b).

Oscillation studies performed with MAK2-GFP and SO-GFP were conducted as described previously (Fleissner *et al.* 2009b); conidia (0.5×10^7 spores/9-cm plate) from MAK2-GFP or SO-GFP strains were mixed with equal amounts of conidia from the respective deletion mutants and plated on solid VMM, dried, and incubated at 30° for 3–4 hr before being used for microscopy. Images were taken using a Leica SD6000 microscope with a ×100 1.4 N.A. oil-immersion objective equipped with a Yokogawa CSU-X1 spinning disk head and a 488-nm laser controlled by Metamorph software. Multiple pairs of interacting germlings were analyzed per experiment, and representative pairs are shown for each strain.

Microarray analysis and quantitative RT-PCR

For the PP1 microarray experiment, RNA was isolated from wild-type or Δ*pp-1* conidia grown in constant light at 25° for 3–8 hr in VMM at 25° with constant light. Total RNA from frozen samples was isolated using Zirconia/Silica beads (0.5-mm diameter; Biospec) and a Mini- Beadbeater-96 (Biospec) with 1 ml TRIzol reagent (Invitrogen) according to the manufacturer's instructions. The total RNA was further purified by digestion with TURBO DNA-free (Ambion) and an RNeasy kit (Qiagen). RNA concentration and integrity was checked by Nanodrop and agarose gel electrophoresis.

For the *mak-2*^{Q100G} microarray experiment, strains were grown in liquid VMM for 5 hr at 25° with constant light; 20 min prior to harvesting, cells were treated either with 20 μM 1NM-PP1 in DMSO or with DMSO only.

Microarray hybridization and slide image analysis were as described previously (Tian *et al.* 2007). We chose to use a closed-circuit design for microarray comparisons, which is a statistically robust method of identifying differentially regulated genes over a time series, and used Bayesian Analysis of Gene Expression Levels (BAGEL) (Meiklejohn and Townsend 2005) to determine normalized gene expression values. Microarray profiling data are deposited at the Gene Expression Omnibus (GEO) database (http://www.ncbi.nlm.nih.gov/geo/) as series record GSE46912 (*mak-2* microarray) and GSE49679 (*pp-1* microarray). Genes were clustered based on their differential expression in Δ*pp-1* over the time period using Hierarchical Clustering Explorer 3.0 (de Hoon *et al.* 2004). The MIPS functional catalog (FunCat) was used to assign functional annotation to genes (Ruepp *et al.* 2004). Enrichment of FunCat categories in gene sets *vs.* the whole genome was calculated using hypergeometrix distribution for *P*-value calculation.

Quantitative RT-PCR was used to confirm trends in the microarray and RNA-seq data, and was performed using the EX-PRESS One-Step SYBR GreenER Kit (Invitrogen) and the StepOnePlus Real-Time PCR System (Applied Biosystems). Reactions were performed in triplicate with a total reaction volume of 20 μl including 400 nM each of forward and reverse primers and 60 ng template RNA. Data analysis was performed by the StepOne Software (Applied Biosystems), using the Relative Quantitation/Comparative CT (ΔΔCT) setting. Data were normalized to the endogenous control actin. The primers used are listed in Table S1.

RNA-seq

RNA was isolated from conidia grown in constant light for 5 hr in VMM at 25°, originally inoculated at a concentration of 1×10^6 cells/ml. RNA-seq methods were as described in Ellison *et al.* (2011). The protocol used for library construction was modified from the standard Illumina method and

Table 2 Fusion phenotype of strains carrying deletions that showed significant differences in expression level in the *Δpp-1* mutant relative to wild type

NCU ID no.	WT RPKM	Δ*pp-1* RPKM	Protein description	Deletion origin	Fusion % (WT = 86 ± 4)[a]
NCU00309[b]	333	527	Hypothetical	FGSC 19692	WT
NCU00811	1302	630	Hypothetical	This study	WT
NCU00881	145	67	HAM7	13775	0
NCU00995	274	0	Hypothetical	This study	WT
NCU01380	413	1	Hypothetical	This study	WT
NCU01697	130	2	Hypothetical	FGSC 14575	WT
NCU02361	42	117	Formamidase	FGSC 21969	WT
NCU02500	49	642	CCG4	FGSC 14944	WT
NCU03013	368	25	ACW10	FGSC 11222	WT
NCU03960	200	24	HAM12	FGSC 17233	66 ± 6
NCU04122	269	19	Malate dehydrogenase	FGSC 21282	WT
NCU04192	70	42	Vacuolar aspartyl aminopeptidase	FGSC 18884	WT
NCU04732	179	65	HAM11	FGSC 17545 and this study	0
NCU05814	145	48	Hypothetical	FGSC 17770	WT
NCU06698	79	49	Glycogenin	FGSC 12301	WT
NCU07503	77	300	Hypothetical	FGSC 14018	WT
NCU07802	148	1	Hypothetical	FGSC 20487	WT
NCU08332	1422	448	HEX1	Jedd and Chua (2000)	WT
NCU08824	37	73	Molybdopterin-binding domain	FGSC 15980	WT
NCU09560	66	150	Superoxide dismutase	FGSC 21068	WT
NCU09562	501	5	Hypothetical	FGSC 21874	WT
NCU09693	116	5	Hypothetical	This study	WT

[a] Mutants show fusion frequencies similar to their isogenic wild-type parent (FGSC 2489).
[b] Genes in boldface type showed increased expression levels in the Δ*pp-1* mutant.

has been described previously (Ellison *et al.* 2011). An Illumina Genome Analyzer (http://qb3.berkeley.edu/qb3/gsl/index.cfm) was used to sequence reads, and the analysis program TopHat (Langmead *et al.* 2009) was used to process the data. Reads per kilobase mapped (RPKM), a normalized measure of gene expression, were calculated using Cufflinks (Roberts *et al.* 2011). Fisher's exact test was used to test the significance of differences between wild type and Δ*pp-1*, with a significance cutoff of $P < 0.001$. Profiling data (*pp-1* RNA-seq) are deposited at the GEO database (http://www.ncbi.nlm.nih.gov/geo/) series record (GSE50446).

Cell fractionation and Western blotting

Harvested conidia (1×10^6/ml) were inoculated in 100-ml VMM in flasks, incubated for 2.5 hr at 30° with shaking at 200 rpm and then an additional 2.5 hr at 30° without shaking. Germlings were harvested by vacuum filtration over a PVDF membrane and frozen in liquid nitrogen. Protein extraction from ground mycelium was performed using lysis buffer as described in Pandey *et al.* (2004) containing complete protease inhibitors but without phosphatase inhibitor and Triton X-100. Cell fractionation via centrifugation was performed as in Bowman and Bowman (1988). The P1 pellet (vacuoles, mitochondria, and endomembranes) and P2 pellet (plasma membrane) were dissolved in lysis buffer with 1% Triton X-100. The remaining supernatant from P2 was used for immunoprecipitation using Protein G Dynabeads (Invitrogen), according to manufacturer's instructions, with the following exceptions: mouse anti-GFP antibody (Roche) was covalently bound to the beads using BS^3 (Sulfo-DSS, Fisher Scientific) according to manufacturer's instructions. Supernatant samples were incubated with the beads for 3 hr at room temperature. Protein was removed from the beads by heating at 70° for 10 min, and samples were run on a 4–12% Nu-Page Bis-Tris Gel (NOVEX, Life Technologies). Protein gels were subjected to Western blot analysis using standard methods. Samples for the MAK1 and MAK2 phosphorylation Western blot were treated similarly, except, after protein extraction with 1 ml lysis buffer, 25 μl of protein sample was directly loaded on a 7% NuPage Bis-Tris Gel (NOVEX, Life Technologies). Gels were subjected to Western blot analysis using standard methods, and detection of phosphorylated MAK1 and MAK2 was carried out using anti-phospho p44/42 MAP kinase antibodies (1:3000 dilution) (PhosphoPlus antibody kit; Cell Signaling Technology) as described (Pandey *et al.* 2004).

Results

The homeodomain is required for PP1 function

In filamentous fungi, Ste12-like proteins possess two C2H2-Zn^{2+} motifs, in addition to the well-conserved homeodomain-like STE domain (Park *et al.* 2002). The STE domain is essential for function and DNA binding in *S. cerevisiae* (Yuan and Fields 1991). The function of these two domains in *N. crassa* was investigated through the construction of alleles containing point mutations in the DNA-binding motifs. In the first *pp-1* allele, a point mutation (W155C) was made in the STE domain; this residue is in a highly conserved region known to be crucial for homeodomain–DNA interactions (Yuan and Fields 1991). The cysteine

residues within the C2H2-Zn^{2+} motifs are important for DNA-binding activity in zinc-finger transcription factors. We therefore constructed a second *pp-1* allele, in which the two cysteine residues of one of the C2H2-Zn^{2+} motifs were mutated to serine (C623S and C626S); similar mutations in a Ste12-like gene in *C. neoformans* resulted in a strain showing an altered virulence phenotype (Chang *et al.* 2004). In the third *pp-1* allele, the point mutations in both the STE and C2H2-Zn^{2+} motifs were combined to create a double-mutant *pp-1* allele (Figure 1A). These alleles, plus a wild-type *pp-1* allele, were fused to GFP at the C terminus and transformed into the *his-3* locus of a *his-3*; Δ*pp-1* mutant; selection was for His prototrophy (Margolin *et al.* 1997). The wild-type *pp-1* and the *pp-1*$^{C623S;C626S}$ alleles fully rescued the Δ*pp-1* phenotype; strains were indistinguishable from wild type when assessing vegetative growth, cell fusion, female fertility, and ascospore viability (Figure 1B). In contrast, strains bearing the *pp-1*^{W155C} allele or the *pp-1*$^{W155C;C623S;C626S}$ allele showed a phenotype identical to the Δ*pp-1* phenotype. These strains showed no cell fusion and were sterile (Figure 1B). These data indicate that the STE domain is essential for all characterized functions of PP1, while the C2H2-Zn^{2+} motif is apparently dispensable.

To assess the phenotypic consequences of overexpression of the wild-type *pp-1* and mutant alleles, the *pp-1*, *pp-1*^{W155C}, and *pp-1*$^{C623S;C626S}$ alleles were cloned behind the *ccg-1* promoter (McNally and Free 1988) and introduced into the Δ*pp-1* strain at the *his-3* locus. Similar to the *pp-1*$^{C623S;C626S}$ strains regulated by the *pp-1* promoter, strains carrying the *pp-1*$^{C623S;C626S}$ allele under the regulation of the *ccg-1* promoter showed a wild-type vegetative, cell fusion, and protoperithecial development phenotype (Figure 1B). However, in contrast to strains bearing the *pp-1*^{W155C} allele regulated by the *pp-1* promoter, strains bearing the *pp-1*^{W155C} allele under the regulation of the *ccg-1* promoter also showed a wild-type vegetative growth phenotype, as well as normal cell fusion levels, protoperithecial development, and ascospore germination. These data suggest that the mutated STE domain can still bind DNA at very low efficiency, which is presumably enough to rescue the Δ*pp-1* phenotype when overexpressed.

PP1-GFP was undetectable when *pp-1-gfp* expression was driven by the native *pp-1* promoter. However, PP1-GFP localized to nuclei during chemotropic interactions and cell fusion when *pp-1-gfp* was expressed from the *ccg-1* promoter (Figure 2A). PP1-GFP driven by the *ccg-1* promoter also showed nuclear localization during colony establishment, vegetative growth, and conidiation (data not shown); differential localization of PP1 during growth or reproduction was not apparent. Nuclear localization was also observed for strains bearing the *pp-1*^{W155C} and *pp-1*$^{C623S;C626S}$ alleles, indicating that these point mutations did not interfere with nuclear localization of PP1.

Transcriptional analysis of PP1 function during early colony development

We used full-genome microarrays (Tian *et al.* 2007) to monitor gene expression profiles in wild-type and Δ*pp-1* during germination, germling fusion, and early establishment of a colony. Gene expression differences between wild type and the Δ*pp-1* mutant were measured 3, 4, 5, 6, and 8 hr following inoculation of conidia into liquid media (Figure 2B). After 3 hr, newly germinated conidia and some chemotropic interactions were observed, which increased over time. Germling fusion events were prevalent after 5 hr, with

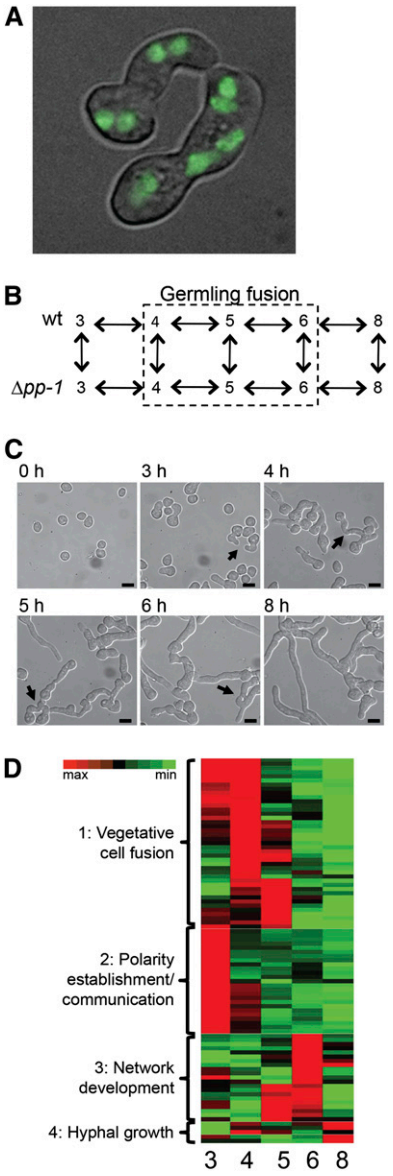

Figure 2 The role of *pp-1* in hyphal network formation. (A) PP1-GFP shows nuclear localization during chemotropic growth in germlings. (B) The closed-circuit experimental design used for microarray analysis. The 4- to 6-hr subpopulation loop is marked in the dashed box. (C) Phenotypic analyses of conidial germination and hyphal network formation in wild type corresponding to identical time points as the 8-hr microarray time course. Arrows denote germling hyphal fusion events. Bar, 10 μm. (D) Visual representation of clustered gene expression profiles from Hierarchical Clustering Explorer analysis (de Hoon *et al.* 2004). Across each horizontal row (representing a single gene from the 3- to 8-hr germination time course), red indicates the highest dependence on PP1 for expression and green indicates the lowest dependence.

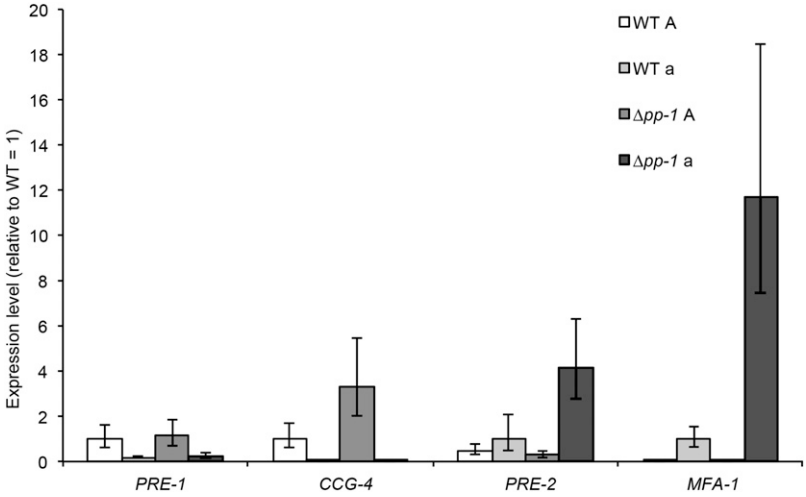

Figure 3 Increased expression of genes encoding mating-type pheromones and receptors in the *Δpp-1* mutant. qRT-PCR was performed on wild-type mating type *A* (FGSC 2489), wild-type mating type *a* (FGSC 988), and Δ*pp-1 A* and Δ*pp-1 a* strains, 5 hr post-inoculation.

~85% of conidia having undergone fusion events by this time point. Hyphal growth and branching started after 6 hr post-inoculation, and elongated and branched hyphae were abundant at 8 hr (Figure 2C).

A total of 5114 genes showed measurable expression levels throughout the time course, but only 92 genes showed expression at all time points and statistically significant expression differences of at least 1.5-fold between wild type and the Δ*pp-1* mutant at one or more time points (Table S2). Consistent with its role as a transcriptional activator, >50% of the genes showed decreased expression levels in the Δ*pp-1* mutant as compared to those with increased expression levels (60 down-regulated *vs*. 32 up-regulated).

Hierarchical clustering of the 92 genes during the 3- to 8-hr time course revealed four distinct clusters (Figure 2D; Table S2). The largest cluster of genes (cluster 1) showed differential expression levels during the 3- to 5-hr time course, when the process of chemotropic interactions and germling fusion events is most prevalent. A second cluster (cluster 2) showed differential expression specifically at the first time point (3 hr), suggesting that these genes may be important for the conidial germination process. The third and the fourth clusters showed differential expression during the 6- to 8-hr time course, suggesting that these genes are involved in the network formation and hyphal growth processes.

ccg-4, which encodes the mating type *A* pheromone, showed increased expression levels in a mating type *A* Δ*pp-1* mutant as compared to a wild-type mating type *A* strain (FGSC 2489) (Table S2). Increased expression levels of *ccg-4* were also reported using partial genome microarrays and Δ*pp-1 A* and Δ*mak-2 A* strains (Li *et al.* 2005). We confirmed this observation by quantitative RT-PCR (qRT-PCR) from wild type *A* and Δ*pp-1 A* strains (Figure 3). However, in mating type *a* strains as well as in Δ*pp-1 a* strains, expression of *ccg-4* was very low. We therefore also evaluated the expression of the mating type *a* pheromone gene, *mfa-1*, in wild type *A* and *a* strains, as well as in Δ*pp-1 A* and *a* mating type strains; *mfa-1* expression levels were significantly higher in the Δ*pp-1 a* cells as compared to a wild-type *a* strain (Figure 3). To determine whether mutations in Δ*pp-1* also affect expression of the pheromone receptors, we assessed expression levels of *pre-1* (*a* pheromone receptor) and *pre-2* (*A* pheromone receptor) by performing qRT-PCR with mating type *A* and *a* Δ*pp-1* mutants as compared to wild-type mating type *A* and *a* strains. While expression levels for *pre-1* were not significantly different between wild type and either *A* or *a* Δ*pp-1* cells, expression levels for *pre-2* showed increased expression levels in the Δ*pp-1 a* mating type strain (Figure 3).

To identify additional genes whose expression correlated with germling fusion events, we assessed expression differences using a subset of the time course, 4–6 hr, as some genes involved in colony development may not be expressed at either 3 or 8 hr, and our statistical analysis method requires data at all time points (see *Materials and Methods*). From analyzing data from the 4- to 6-hr loop, we identified an additional 26 genes (for a total of 86 genes) that showed decreased expression levels and 9 genes (for a total of 41 genes) that showed increased expression levels in the Δ*pp-1* mutant relative to wild type (Figure 4, A and B; Table S2). Together with genes identified from the 3- to 8-hr time course, FunCat analysis showed that most of the genes with lower expression in the Δ*pp-1* strain belonged to unclassified/hypothetical proteins (Table S3). Additional overrepresented categories included various signaling pathways and vacuolar degradation ($P < 0.05$; Table S3). Of the genes that showed increased expression in the Δ*pp-1* strain, enrichment for the functional category of transcription was identified ($P < 0.05$; Table S4).

RNA-seq analyses were performed as a more sensitive method to identify transcriptional differences between wild-type and Δ*pp-1* cells at the time point with the highest number of germling fusion events, 5 hr post-inoculation. After statistical analysis (*Materials and Methods*), a total of 548 genes were identified as being significantly differentially expressed by at least 1.5-fold between wild type and

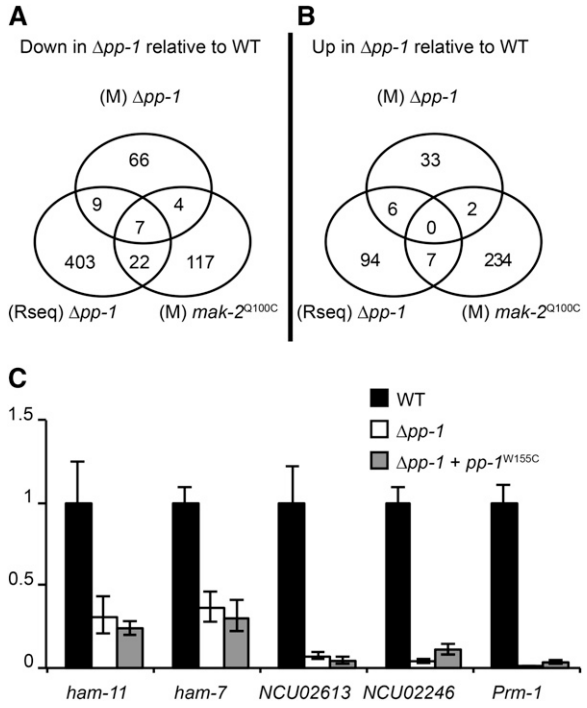

Figure 4 Summary of microarray and RNA-seq profiling data on Δ*pp-1* and *mak-2*^{Q100G} mutants relative to wild type. (A) Venn diagram showing the overlap of genes that demonstrated a decrease in expression level identified by Δ*pp-1* (M Δ*pp*-1) and *mak-2*^{Q100G} (M *mak-2*^{Q100G}) microarrays and RNA-seq analysis (Rseq Δ*pp-1*) as compared to their wild-type isogenic parent (FGSC 2489). (B) Venn diagram showing the overlap of genes that demonstrated an increased expression level in the Δ*pp-1* (M Δ*pp*-1) and *mak-2*^{Q100G} (M *mak-2*^{Q100G}) and RNA-seq analysis (Rseq Δ*pp-1*) as compared to their isogenic wild-type parent (FGSC 2489). (C) qRT-PCR analysis showing relative expression levels of genes identified as being differentially expressed via microarrays/RNA-seq in the Δ*pp-1* and Δ*pp-1* + *pp-1*^{W155C} mutants relative to wild type (FGSC 2489).

Δ*pp-1*; 441 genes showed reduced expression levels in the Δ*pp-1* mutant while 107 genes showed increased expression levels as compared to wild type (Figure 4, A and B; File S1).

Transcriptional analyses of MAK-2 function during early colony development

A Δ*mak-2* mutant in *N. crassa* shows a very similar phenotype to a Δ*pp-1* mutant, including lack of cell fusion, reduced vegetative growth, female sterility, and ascospore lethality (Pandey *et al.* 2004; Li *et al.* 2005). The question of whether MAK2 kinase activity is required for MAK2 oscillation, as well as for the oscillation of a second protein, SO, which is also required for cell fusion (Fleissner *et al.* 2009b), was tested by constructing a *mak-2* allele (*mak-2*^{Q100G}) containing a point mutation that allows specific inhibition of kinase activity with an ATP analog (1NM-PP1; Fleissner *et al.* 2009b). Addition of the inhibitor 1NM-PP1 to *mak-2*^{Q100G} cells undergoing communication immediately blocks further oscillation of both MAK2 and SO and abruptly abolishes chemotropic interactions (Fleissner *et al.* 2009b). As a complement to our transcriptional profiling of the Δ*pp-1* mutant, and to identify targets more specifically related to the MAK2 kinase cascade, we performed transcriptional analysis of *mak-2*^{Q100G} cells at the 5-hr time point, with and without exposure to 1NM-PP1, for the final 20 min of their growth (see *Materials and Methods*). We identified 392 genes with modified expression (≥1.5-fold) in the 1NM-PP1 *mak-2*^{Q100G}-treated cells *vs. mak-2*^{Q100G} (DMSO only). Of these, 149 genes showed a decreased expression level *vs.* 243 genes that showed increased expression levels (Figure 4, A and B; File S2). FunCat analysis of genes showing an increased expression level also showed an overrepresentation ($P < 0.01$) in categories of metabolism and in categories related to transport and defense (File S2), suggesting that treatment with 1NM-PP1 may elicit defense responses in *N. crassa*. Within the genes that showed decreased levels of expression was *mak-2* itself, suggesting a feedback mechanism initiated as a result of the stalled signaling.

In total, 22 genes were identified as PP1 targets via both the microarray and the RNA-seq analyses, and an additional 6 genes were identified with the inclusion of the *mak-2*^{Q100G} microarray data (Figure 4, A and B; Table S4). Altogether, 7 genes were identified in all three experiments, including *ham*-7 (NCU00881), a previously identified gene required for hyphal fusion (Fu *et al.* 2011; Maddi *et al.* 2012); NCU04122 (malate dehydrogenase); and 5 genes encoding the predicted hypothetical proteins NCU00995, NCU01697, NCU03960, NCU04732, and NCU09693. Genes encoding five additional hypothetical proteins were identified in the overlap between the Δ*pp-1* microarray and RNA-seq data (NCU00811, NCU01380, NCU05814, NCU07802, and NCU09562) as well as an anchored cell-wall protein (*acw-10*) (Maddi *et al.* 2009); *hex-1*, which encodes a protein involved in septal plugging (Jedd and Chua 2000); glycogenin (NCU06698); and vacuolar aspartyl aminopeptidase (NCU04192). In the comparison between the down-regulated genes in the Δ*pp-1* microarray and the *mak-2*^{Q100G} microarray, only one additional gene encoding a hypothetical protein was identified (NCU07439). In the gene set that overlapped between the Δ*pp-1* RNA-seq data and the *mak-2*^{Q100G} array data (decreased expression category), 5 additional genes were identified that, when mutated, resulted in strains blocked in germling/hyphal fusion. These include two components of the NADPH oxidase regulatory system, *nox-1* (NCU02110) and *nor-1* (NCU07850) (Fleissner *et al.* 2008; Fu *et al.* 2011); a transcription factor, *adv-1* (NCU07392) (Fu *et al.* 2011); *ham-6* (NCU02767), encoding a predicted transmembrane protein (Fu *et al.* 2011); and *Prm-1*. *Prm-1* is involved in plasma membrane merger in *N. crassa* during both vegetative and sexual cell fusion (Fleissner *et al.* 2009a).

To confirm expression differences between Δ*pp-1* and wild type, we used qRT-PCR to analyze the expression of six genes, two from the set of seven overlapping genes from all three experiments, NCU04732 and *ham-7* (NCU00881); two genes identified from the RNA-seq analysis, NCU02613 (hypothetical) and NCU02246 (hypothetical); and *Prm-1* (NCU09337), which was identified in both the RNA-seq

Table 3 Previously identified cell fusion genes that showed dependence on *pp-1* for wild-type expression levels in germlings

Gene	Locus ID no.	Gene description	Reference
Prm-1	NCU09337	Membrane protein	Fleissner *et al.* (2009a)
mek-1	NCU06419	MAP kinase kinase	Fu *et al.* (2011)
ham-6	NCU02767	Small hydrophobic protein	Fu *et al.* (2011)
so	NCU02794	WW domain protein	Fleissner *et al.* (2005)
ham-8	NCU02811	Transmembrane protein	Fu *et al.* (2011)
nox-1	NCU02110	NADPH oxidase	Cano-Dominguez *et al.* (2008)
ham-9	NCU07389	Plekstrin domain protein	Fu *et al.* (2011)
ham-7	NCU00881	GPI-anchored protein	Fu *et al.* (2011); Maddi *et al.* (2012)
adv-1	NCU07392	Transcription factor	Fu *et al.* (2011)
gpip-2	NCU07999	GPI-anchored protein	Bowman *et al.* (2006)
nor-1	NCU07850	NADPH oxidase regulator	Cano-Dominguez *et al.* (2008)
gpip-1	NCU06663	GPI-anchored protein	Bowman *et al.* (2006)
mak-1	NCU09842	MAP kinase	Fu *et al.* (2011); Maddi *et al.* (2012)
pp2A	NCU06563	Catalytic subunit of protein phosphatase 2A	Fu *et al.* (2011)
mob-3	NCU07674	Phocein	Maerz *et al.* (2009)
rco-1	NCU06205	Transcription factor	Aldabbous *et al.* (2010)

and *mak-2*^{Q100G} microarray analyses. Our qRT-PCR recapitulated our RNA-seq/microarray analyses (Figure 4C), with the expression of all identified target genes being significantly reduced in both the Δ*pp-1* and *pp-1*^{W155C} mutants relative to wild type.

PP1 and the regulation of genes required for hyphal fusion and network development

Approximately 40 genes have been identified with roles in colony establishment in *N. crassa*, specifically during germling or hyphal fusion (see review in Read *et al.* 2010, 2012). By evaluating our expression data, 16 of these genes were dependent on PP1 for their expression (>1.5-fold lower in Δ*pp-1* as compared to WT, $P < 0.05$, RNA-seq data) (Table 3). This list included *ham-7*, *Prm-1*, *ham-6*, *nox-1*, *nor-1*, and *adv-1*, as well as 2 genes encoding kinases in the cell-wall integrity pathway (*mek-1* and *mak-1*) (Read *et al.* 2010); 2 genes encoding predicted components of the striatin complex (*pp2A* and *mob-3*) (Maerz *et al.* 2009; Fu *et al.* 2011); one transcription factor (*rco-1*) (Aldabbous *et al.* 2010); genes for two GPI-anchored cell-wall proteins (*gpip-2* and *gpip-1*) (Bowman *et al.* 2006); *ham-8*, encoding a predicted transmembrane protein; *ham-9*, encoding a protein with pleckstrin homology domain and a sterile α-motif domain (Fu *et al.* 2011); and *so* (Fleissner *et al.* 2005). During germling fusion, SO also oscillates to CAT tips, with opposite dynamics to MAK2 (Fleissner *et al.* 2009b); correct oscillation of SO requires MAK2 kinase activity.

Identification of novel proteins involved in hyphal fusion and network development

A comparison of the Δ*pp-1* microarray and RNA-seq analyses identified a 16-gene overlap that showed reduced expression levels, and a 6-gene overlap that showed increased expression levels, in the Δ*pp-1* mutant relative to wild type (Figure 4 and Table 2). We therefore evaluated the germling fusion/colony establishment phenotypes of strains containing deletions of these genes. Of these 22 genes, 18 deletion mutants were available from the FGSC (McCluskey 2003), and we constructed strains carrying deletions for the remaining 4 genes (NCU00811, NCU0995, NCU01380, and NCU09693) (Table 2). Germling fusion frequency of each deletion strain was determined and compared to the wild-type isogenic parent. Of the 22 deletion strains assayed, three mutants were affected in the ability to undergo germling fusion. As expected, *ham-7* (NCU00881) mutants were completely unable to undergo germling fusion (Fu *et al.* 2011), and in addition so was a mutant carrying a deletion of NCU04732, which encodes a hypothetical protein (Figure 5A). Deletion of an additional gene, NCU03960, which also encodes a hypothetical protein, resulted in a strain that was capable of fusion, but with a significantly lower fusion frequency than wild type (Table 2 and Figure 5A).

NCU04732 was named *ham-11*. HAM11 is a 633-amino-acid protein with two predicted transmembrane domains and is highly conserved among the Sordariomycetes. However, predicted proteins with strong homology in the N- and C-terminal regions to HAM11 were present in the genomes of most filamentous ascomycete species (no homologs were detected in Saccharomycetes or in Basidiomycetes). The Δ*ham-11* mutants were fully fertile as a male or as a female, indicating that HAM11 is specifically required for germling fusion and not for sexual fusion. The Δ*ham-11* growth phenotype differs from other fusion mutants (Δ*mak-2*, Δ*so*, and Δ*ham-7*) in that colonies were not "flat" due to reduced aerial hyphae extension (Figure 5, B and C). Aerial hyphae extension in Δ*ham-11* mutants was similar to wild type (17 mm ± 1.7 as compared to 18.2 mm ± 2.6 for wild type), while aerial hyphae extension in Δ*ham-7* mutants was only 1/2 of wild type (11 mm ± 1.3). The growth rate of Δ*ham-11* over 48 hr was slightly slower than for wild type (Figure 5D).

A strain carrying a deletion of NCU03960, hereafter called *ham-12*, showed a significant (Student's *t*-test: $P <$

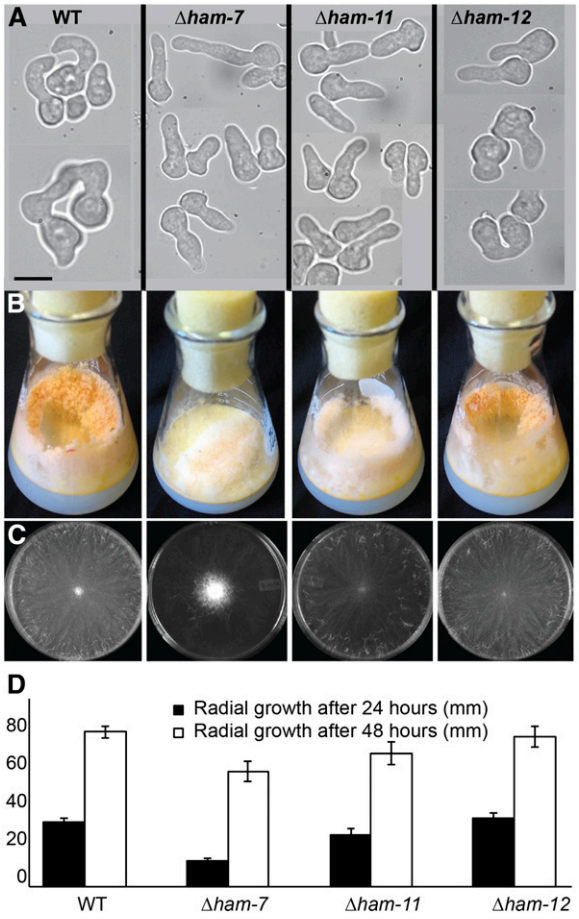

Figure 5 Fusion phenotypes of deletion mutants in PP1 target genes. (A) Chemotropic interactions and CAT fusion phenotypes of wild type (FGSC 2489), compared to the isogenic mutant strains Δ*ham-7*, Δ*ham-11*, and Δ*ham-12*. (B) Macroscopic growth phenotype of wild type, Δ*ham-7*, Δ*ham-11*, and Δ*ham-12* mutants in flasks. Note the shortened aerial hyphae in the Δ*ham-7* mutant. (C) Macroscopic growth phenotype on VMM plates of wild type, Δ*ham-7*, Δ*ham-11*, and Δ*ham-12* 2 days post-inoculation. (D) Radial growth (in mm) of wild type, Δ*ham-7*, Δ*ham-11*, and Δ*ham-12* mutants over a 48-hr time period.

0.01) reduction in fusion frequencies as compared to wild type (66 *vs.* 87%, respectively) (Table 2). *ham-12* is predicted to encode a 157-amino-acid protein with one predicted transmembrane domain, but without any annotated function. *ham-12* is more highly conserved than *ham-11*, with homologs identified across filamentous ascomycete fungi (Pezizomycotina). The growth, reproductive phenotype, and aerial hyphae extension of the Δ*ham-12* mutant were identical to wild type (Figure 5, B–D).

Fusion defect of Δham-11 germlings is suppressed in the presence of a wild-type partner cell

When wild-type germlings communicate, MAK2 oscillates from the cytoplasm to CAT tips every 4 min (8 min/cycle; Figure 6A). Similarly, when wild-type germlings communicate, SO oscillates from the CAT tips to the cytoplasm every 4 min (Figure 7A); MAK2 and SO oscillate in perfect opposition during chemotropic interactions (Fleissner *et al.* 2009b). To determine whether Δ*ham-7* or Δ*ham-11* germlings show an altered oscillation pattern of MAK2, we introduced *mak-2-GFP* constructs into wild type, Δ*ham-7*, and Δ*ham-11* strains. For both Δ*ham-7* and Δ*ham-11* germlings, localization of MAK2-GFP was cytoplasmic, and localization to germling tips, chemotropic interactions, or cell fusion was not observed (Figure 6B and Figure 8). However, when Δ*ham-11* germlings were confronted with wild-type cells, chemotropic interactions and cell fusion were observed. However, the percentage of Δ*ham-11* germlings communicating with wild type was ~25% lower as compared to wild-type–wild-type interactions, as wild-type–type fusions were overrepresented in mixtures of Δ*ham-11* + wild-type germlings.

We hypothesized that in wild-type + Δ*ham-11* germling pairs where chemotropic interactions were observed, MAK2 oscillation would be restored. As predicted, oscillation of MAK2-GFP in wild-type cells, when confronted with Δ*ham-11* germlings, was identical to wild-type + wild-type pairings and showed identical MAK2 oscillation dynamics (8-min cycle from CAT tip to cytoplasm) (Figure 6C). Similarly, when Δ*ham-11* germlings bearing MAK2-GFP were in proximity to wild-type cells, oscillation of MAK2 was coincident with chemotropic interactions and cell fusion (Figure 6D). In contrast, Δ*ham-11 mak-2-gfp* + Δ*ham-11* germlings showed only cytoplasmic localization of MAK2 (Figure 6B). In contrast to the results obtained with Δ*ham-11* mutants, no chemotropic interactions were observed between wild-type + Δ*ham-7* germlings, and oscillation of MAK2 to CAT tips was not apparent in wild-type cells in proximity to Δ*ham-7* germlings, nor in Δ*ham-7* germlings bearing MAK2-GFP in proximity to wild-type cells (Figure 8).

We hypothesized that SO oscillation would also be restored in wild type + Δ*ham-11* germlings when chemotropic interactions and cell fusion were observed. As predicted, SO oscillated in an 8-min cycle from CAT tip to cytoplasm in wild-type cells bearing SO-GFP communicating with Δ*ham-11* cells (Figure 7C) and also when Δ*ham-11* germlings bearing SO-GFP were undergoing chemotropic interactions with wild-type cells (Figure 7D). The dynamics of SO oscillation in wild type + Δ*ham-11* pairings showed identical dynamics to wild-type + wild-type pairings. The phenotype of the Δ*ham-11* mutant is unique among fusion mutants: communication and fusion are not restored when other fusion mutants are confronted with wild-type strains (mutants are unable to send or receive fusion signals) (Xiang *et al.* 2002; Pandey *et al.* 2004; Fleissner *et al.* 2005; Simonin *et al.* 2010; Fu *et al.* 2011).

Some fusion mutants are impaired in proper phosphorylation of the two MAPK kinases, MAK1 or MAK2, which are both required for germling fusion (Dettmann *et al.* 2012; Maddi *et al.* 2012). Since the Δ*ham-11* mutant failed to initiate chemotropic interactions, we also evaluated phosphorylation of MAK1 and MAK2 in Δ*ham-11* germlings with the Δ*ham-7* mutant as a control. Conidia from wild type, Δ*ham-7*, or Δ*ham-11* were germinated for 5 hr, and total

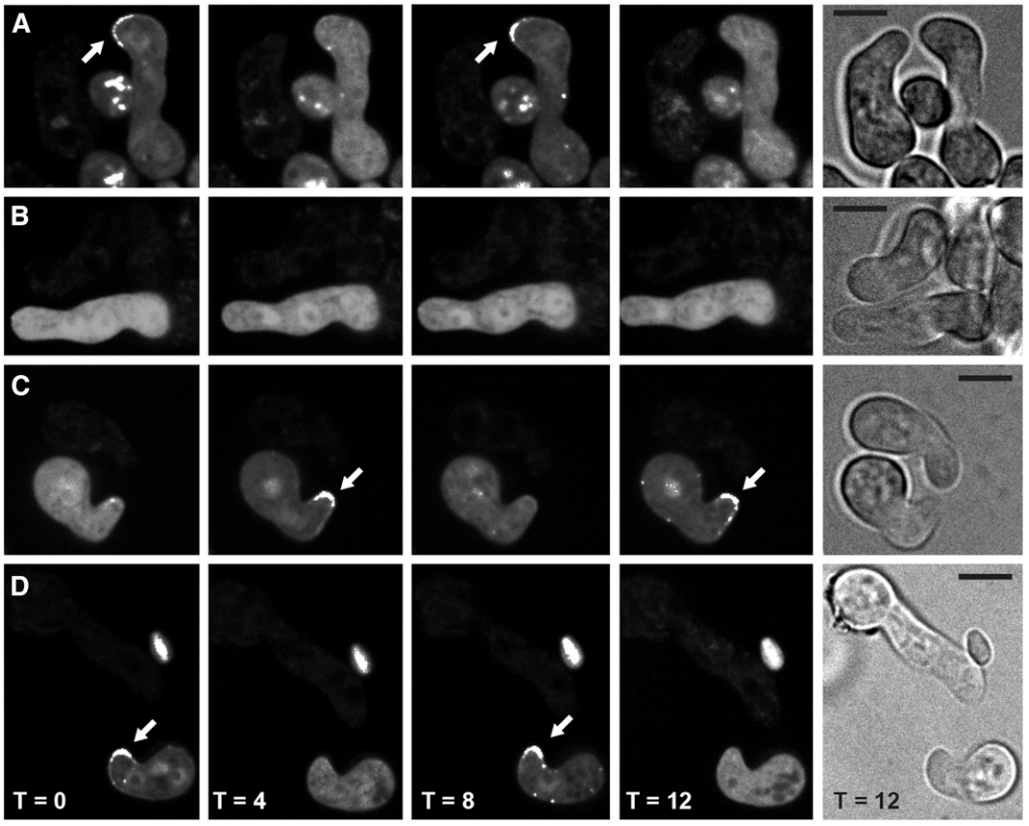

Figure 6 Localization of MAK2-GFP in wild type (FGSC 2489; WT) and Δ*ham-11* during germination and germling interactions. (A) MAK2-GFP oscillates to the tip every 8 min (arrows) in a wild-type cell bearing MAK2-GFP when communicating with an otherwise isogenic wild-type germling (WT *mak-2-gfp* + wild type). (B) MAK2-GFP shows no oscillation in Δ*ham-11 mak-2-gfp* germlings in proximity to otherwise isogenic Δ*ham-11* cells (Δ*ham-11 mak-2-gfp* + Δ*ham-11*). (C) Chemotropic interactions and MAK2-GFP oscillation are apparent when wild-type germlings bearing MAK2-GFP are in proximity to Δ*ham-11* germlings (WT *mak-2-gfp* + Δ*ham-11*). (D) Oscillation of MAK2-GFP is apparent in Δ*ham-11* germlings in proximity to wild-type cells (Δ*ham-11 mak-2-gfp* + WT). Arrows indicate localization of MAK2-GFP to CAT tips when observed. Bright-field pictures on right show both germlings. Bar, 10 μm.

protein was extracted and subjected to Western blot using phospho-specific P22/P24 antibodies, which recognize phosphorylated MAK1 and MAK2. As previously described (Maddi *et al.* 2012), Δ*ham-7* shows a defect in phosphorylation of MAK1 and, to a modest extent, phosphorylation of MAK2. Surprisingly, Δ*ham-11* germlings showed wild-type levels of phosphorylation of both MAK1 and MAK2 (Figure 9). These data indicate that, even though MAK2 oscillation to CAT tips is defective in Δ*ham-11* germlings, phosphorylation of MAK2 by upstream factors is not.

We constructed *gfp*-tagged alleles of *ham-11* driven by the *tef-1* promoter to determine localization of HAM11 in cells undergoing chemotropic interactions *vs.* those that are not communicating. The *tef-1* gene is more highly expressed in germlings than *ccg-1* and has been used to localize NCR1 and MEK2 to CAT tips (Dettmann *et al.* 2012). GFP was fused within the *ham-11* ORF between amino acids 62 and 63, which lie between the two predicted transmembrane domains. This construct was transformed into a *his-3*; Δ*ham-11* strain. Complementation was assessed in homokaryotic *his-3*::*ham-11-gfp*; Δ*ham-11* progeny via evaluating germling fusion frequencies. In contrast to the Δ*ham-11* strain that lacks germling fusion, germlings of the *his-3*::*ham-11-gfp*; Δ*ham-11* strain showed fusion frequencies similar to wild-type + wild-type pairings (Figure 9A). However, although HAM11 could be detected via Western analyses, GFP fluorescence in live cells could not be detected above background.

Because we could detect HAM11 via Western blotting, but not by fluorescence microscopy, we resorted to cell fractionation to determine HAM11 localization. As a control, we utilized PRM1-GFP, which localizes to the plasma membrane and to internal membrane-bound structures (Fleissner *et al.* 2009a). We evaluated the presence of HAM11 and PRM1 during germling fusion (5-hr time point). From the cell lysate, three fractions were obtained: a resolubilized pellet containing endomembranes, a second resolubilized pellet containing plasma membranes, and a supernatant fraction from which cytoplasmic GFP-protein was immunoprecipitated. Antibodies to the *N. crassa* plasma membrane ATPase, which localizes to the plasma membrane (Bowman and Bowman 1988), were used to assure proper fractionation (data not shown). As expected, PRM1-GFP was observed in fractions containing membranes (endomembranes and plasma membrane), but not in the cytoplasmic fraction (Figure 9B), consistent with fluorescence mircroscopy results (Fleissner *et al.* 2009a). HAM11-GFP, however, was found in all three cellular fractions (Figure 9B). These data suggest that HAM11 is a protein that can shuttle between cytoplasm and vesicles/membranes in the cell.

Discussion

The MAK2 MAPK pathway in *N. crassa* is required for chemotropic interactions and cell fusion during vegetative growth. In this study, we show that one of the predicted targets of the MAK2 pathway, the transcription factor PP1, is also required for chemotropic interactions. This strongly supports the role of PP1 as a target of this MAPK pathway

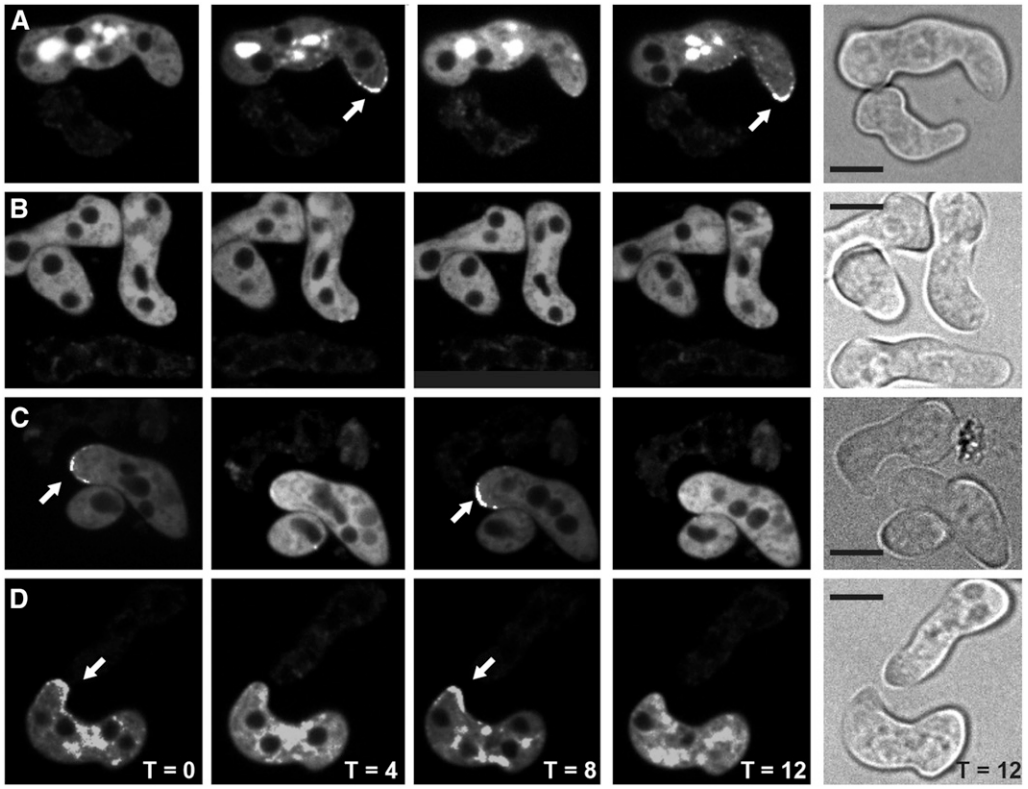

Figure 7 Localization of SO-GFP in wild-type and Δ*ham-11* germlings. (A) A time course of SO-GFP oscillation during chemotropic interactions between wild-type germlings; oscillation of SO-GFP to CAT tips occurs every 8 min (WT *so-gfp gfp* + WT). (B) Δ*ham-11* germlings bearing SO-GFP lack oscillation and localization of SO-GFP to CAT tips when in proximity to other Δ*ham-11* germlings (Δ*ham-11 so-gfp-gfp* + Δ*ham-11*). (C) Wild-type cells bearing SO-GFP show oscillation when in proximity to Δ*ham-11* cells and chemotropic interactions are restored (WT *so-gfp* + Δ*ham-11*). (D) Δ*ham-11* germlings bearing SO-GFP show chemotropic interactions and oscillation of SO-GFP to CAT tips when in proximity to wild-type germlings (Δ*ham-11 so-gfp* + WT). Note that the oscillation dynamics of SO-GFP are identical to the WT + WT germling interactions shown in A. Arrows show localization of SO-GFP to CAT tips. Bright-field pictures show germlings. Bar, 10 μm.

during cell fusion. We subsequently utilized a combination of transcriptional approaches during a time of intensive chemotropic interactions and germling fusion events to identify new components of the cell fusion pathway. When comparing the three data sets (Δ*pp-1* and Δ*mak-2*^{Q100G} microarrays and Δ*pp-1* RNA-seq), we identified an overlapping set of seven genes that contained three whose deletion affected germling fusion frequency. These included a previously identified fusion gene of unknown biochemical function (*ham-7*), which encodes a GPI-anchored protein. Recent data implicate HAM7 in functioning as a cell-wall sensor to regulate activation of the cell-wall integrity MAPK MAK1 (Maddi *et al.* 2012). Strains carrying a deletion of *mak-1* show a pleiotropic phenotype and are also unable to undergo chemotropic interactions and germling fusion (Fu *et al.* 2011). Of the ~40 genes that have been previously identified as being required for germling fusion, 15 were identified within our gene set that showed a reduction in expression level in Δ*pp-1* or *mak-2*^{Q100G} strains, particularly in the Δ*pp-1* RNA-seq data set, reflecting the increased power of expression detection over traditional microarray data. In addition to genes that were coordinately regulated in the *mak-2*^{Q100G} and the Δ*pp-1* data sets (genes up in both mutants or down in both mutants), genes that showed opposite regulation (increased expression level in one mutant was correlated with decreased expression in the second mutant) were also identified. In *S. cerevisiae*, Fus3p regulates negative effectors of Ste12p (Dig1p and Dig2p), in addition to direct regulation of Ste12p (Elion *et al.* 1993; Tedford *et al.* 1997; Blackwell *et al.* 2007), with activation of Fus3p being correlated with activation of Ste12p. In *N. crassa*, MAK2 also shows nuclear localization in germlings (Fleissner *et al.* 2009b), suggesting that MAK2 may influence activity of transcription factors in addition to PP1. Additional intricacies of PP1 regulation by MAK2 may occur in *N. crassa* as well as in other filamentous fungi, and gene sets that showed opposite expression patterns in the *Δmak-2* mutant *vs.* the *Δpp-1* mutant offer a opportunity to explore this issue.

In addition to their role in germling fusion, it is clear that both PP1 and MAK2 are important in coordinating germination and hyphal growth. This aspect is also true for many of the previously identified fusion mutants, such as Δ*ham-2*, Δ*ham-3*, Δ*ham-4*, and Δ*ham-7* (Xiang *et al.* 2002; Simonin *et al.* 2010; Fu *et al.* 2011), which also have pleiotropic phenotypes. Thus, our data may also be useful in the identification of components important for these processes in filamentous fungi, such as *N. crassa*. For example, in *S. cerevisiae*, Ste12 is important for invasive growth in haploid cells, while in diploid cells it plays a role in filamentation that occurs in response to nitrogen starvation (Gustin *et al.* 1998; Gancedo 2001). It is noteworthy that, in all our transcriptional profiling data sets during germination and colony establishment, the category showing the largest enrichment was that of unclassified proteins. This observation underscores our lack of understanding of developmental processes unique to filamentous fungi.

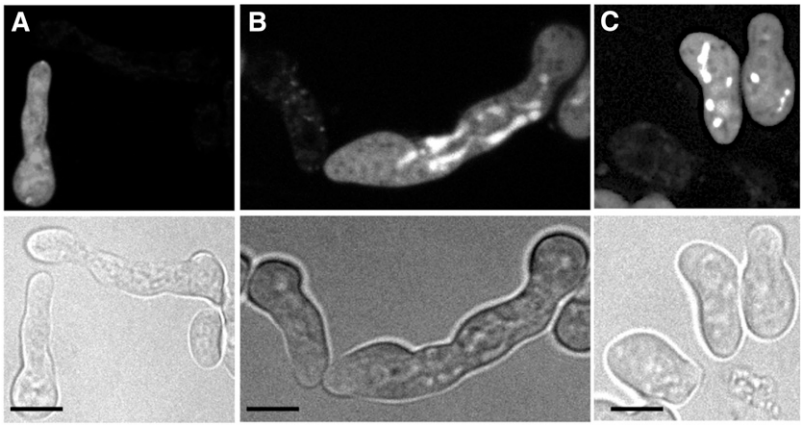

Figure 8 Lack of oscillation of MAK2-GFP and chemotropic interactions in Δ*ham-7* germlings in proximity to wild type. (A) Cytoplasmic localization of MAK2-GFP in wild-type germlings when in proximity to Δ*ham-7* germlings (WT *mak-2-gfp* + Δ*ham-7*). No oscillation of MAK2-GFP was observed during the time course. (B) Cytoplasmic localization of MAK2-GFP and lack of chemotropic interactions when *mak-2-gfp*; Δ*ham-7* germlings are in proximity with wild-type cells (WT + Δ*ham-7 mak-2-gfp*). No localization of MAK2-GFP to CAT-like structures was observed during the time course. (C) Lack of chemotropic interactions between Δ*ham-7* germlings and cytoplasmic localization of MAK2-GFP (Δ*ham-7* + Δ*ham-7 mak-2-gfp*). Bright-field pictures show the germling proximity. Bar, 10 μm.

MAPK pathways orthologous to MAK2 have been implicated in sexual development in filamentous fungi; Δ*pp-1* and Δ*mak-2* mutants fail to form female reproductive structures but are fully fertile as males (although both display an ascospore germination defect). Surprisingly, we found a mating-type-specific effect on the expression of the mating pheromones, *ccg-4* (*A* pheromone; up in Δ*pp-1 A*) and *mfa-1* (*a* pheromone; up in Δ*pp-1 a*), and to a lesser extent the mating-type pheromone receptor, *pre-2* (*A* pheromone receptor; up in Δ*pp-1 a*). These data suggest interplay between the *A* and *a* mating-type-specific transcription factors believed to regulate pheromones and receptors in *N. crassa* (*A-1* and *a-1*) and PP1. Pheromones (expressed by male cells) and receptors (expressed by trichogynes undergoing chemotropic interactions toward a male cell) are essential for mating in *N. crassa* (Kim and Borkovich 2004, 2006). In the closely related homothallic ascomycete fungus, *S. macrospora*, STE12 binds the mating-type protein SMTA-1, a small serine-threonine protein, SIP2, and the MADS box protein MCM1 during formation of reproductive structures (Nolting and Poggeler 2006). However, deletion of *ste12* in *S. macrospora* does not affect vegetative growth or fruit body development. In *S. cerevisiae*, Ste12 via interaction with Mcm1 induces **a**-specific genes in response to pheromone activation, while Mcm1, α1, and Ste12 induce α-specific genes (Errede and Ammerer 1989; Yuan *et al.* 1993). Further experiments are needed to understand the interplay of PP1, the mating-type-specific transcription factors, pheromones, and receptors during both vegetative and sexual reproduction.

Ste12-like transcription factors are highly conserved among filamentous fungi. A comparison of our transcriptional data set with Ste12 chromatin-immunoprecipitation data from *S. cerevisiae* (Ren *et al.* 2000; Borneman *et al.* 2007; Zheng *et al.* 2010) identified nine conserved genes, including *STE12/pp-1*, *FUS3/mak-2*, *PHD1/Asm-1* (NCU01414) (transcriptional activator), *PRM1/Prm-1* (plasma membrane merger), *ACO1/*NCU02366 (aconitase), *PGU1/*NCU02369 (endopolygalacturonase), *CHS1/chs-3* (chitin synthase), *HAA1/*NCU04830 (transcriptional activator), and *PCL2/* NCU04847 (cyclin) that were conserved. Of these genes, mutations in three affect germling fusion in *N. crassa*: *pp-1*, *mak-2*, and *Prm-1*. Interestingly, preliminary data show that a strain carrying a deletion of *Asm-1* is also a hyphal fusion mutant (data not shown). An *Asm-1* mutant shows a vegetative ("flat") phenotype, female sterility, and an ascospore maturation defect (Aramayo *et al.* 1996), phenotypes that are reminiscent of Δ*pp-1*. In *S. cerevisiae*, the Ste12-binding motif is TGAAACA, although not all target genes identified in *S. cerevisiae* show conservation of these sites (Ren *et al.* 2000; Borneman *et al.* 2007; Zheng *et al.* 2010). In *N. crassa*, only between 4–6.5% of the genes identified in the 1NM-PP1 MAK2^{Q100G} and PP-1 RNA-seq experiments have a STE12-like motif present in their promoters at high confidence (data not shown). However, transcription-factor-binding sites are short and often degenerate, making computational detection in promoter regions of genes across an entire genome difficult (Tompa *et al.* 2005). Future experiments using ChIP-seq analyses would clarify direct target genes of PP1, especially if performed under different growth and developmental scenarios.

Of the seven genes that overlapped from all the expression profiling data sets, a deletion of one of them, *ham-11*, resulted in a phenotype that is unique among fusion mutants. All fusion mutants identified so far are blind and do not respond to the presence of a wild-type partner. The only reported exception is a *N. crassa* mutant in a gene identified by genome-wide association studies of germling communication (Palma-Guerrero *et al.* 2013). In this case, mutations in a predicted secreted protease (*spr-7*) actually increased fusion frequencies (from ∼86% to ∼97%). However, when the Δ*spr-7* mutant was mixed with wild-type germlings, fusion frequency was reduced to wild-type levels. In contrast, germlings of Δ*ham-11* showed no fusion at all, but showed normal chemotropic interactions; oscillations of MAK2 and SO and near wild-type levels of cell fusion occur when in proximity to wild-type germlings. These data suggest that HAM11 function is essential for the initiation of chemotropic interactions. As *ham-11* was identified as a target of PP1 and the MAK2 pathway, these results suggest a positive feedback mechanism associated with the initiation of signaling. Data showing normal levels of MAK2 phosphorylation

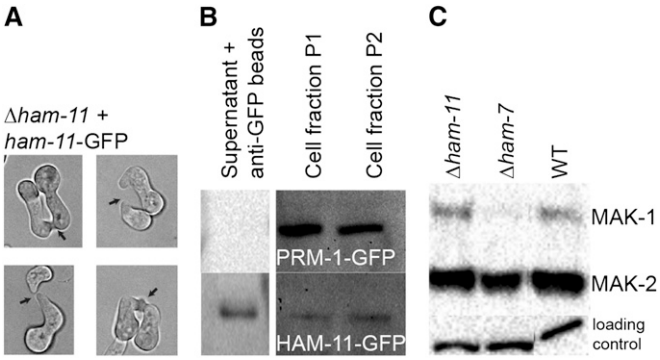

Figure 9 MAK1 and MAK2 phosphorylation, fusion phenotype, and Western blot of Δ*ham-11* complemented with *ham-11-gfp*. (A) Four germling pairs of Δ*ham-11 ham-11-GFP* show chemotrophic growth and cell fusion (see arrows), showing full complementation of the Δ*ham-11* phenotype by the *ham-11-gfp* construct. (B) Western blot of PRM1-GFP (which localizes to endomembranes and the plasma membrane of *N. crassa* by fluorescence microscopy) (Fleissner *et al.* 2009a). HAM11-GFP was detected in supernatant, endomembranes (cell fraction P1), and outer membranes (cell fraction P2). Cell fractionation purity was also assessed using antibodies to the plasma membrane ATPase (data not shown), which localized only to the membrane fractions. (C) Activation of MAK1 and MAK2 in wild type, Δ*ham-11*, and Δ*ham-7* germlings. Protein samples from Δ*ham-11* (lane 1), Δ*ham-7* (lane 2), and wild-type (lane 3) 5-hr-old germlings from liquid VMM are shown. Phosphorylated MAK1 (51 kDa) and MAK2 (41 kDa) were detected using anti-phospho p44/42 MAP kinase antibodies (Cell Signaling Technology). (Bottom) Shows equal loading for each lane.

in the Δ*ham-11* mutant suggest that the defect is associated with the initiation of MAK2 oscillation to CAT tips and that HAM11 is not involved in the upstream cascade leading to MAK2 activation. Cells of *N. crassa* do not initiate chemotropic interactions, nor is localization of MAK2 or SO to CAT tips observed when cells are >15 μm apart. Thus, HAM11 might be involved in the regulation of a switch-like transition to signaling behavior when germlings are close enough to each other to initiate chemotropic interactions. HAM11 was not detected in the extracellular fraction (data not shown), but was identified in both the cytoplasmic and membrane fractions, suggesting that it may shuttle between compartments, perhaps depending upon MAK2-signaling status. Supporting this hypothesis is the finding that HAM11 was identified in a phosphoproteomic study to identify MAK2 substrates (A. Leeder and N. L. Glass, unpublished data).

Most of the fusion mutants previously identified affect chemotropic interactions and signaling of MAK2 and SO. However, a strain carrying a deletion of one of the transcriptional targets identified in this study, *Prm-1*, has normal chemotropic interactions, but is affected in plasma membrane merger (Fleissner *et al.* 2009a). In *S. cerevisiae*, *PRM1* was identified by assessing selectively expressed genes in response to pheromone treatment (Heiman and Walter 2000) and is a direct target of Ste12 (Ren *et al.* 2000); *prm1Δ* mutants are also affected in plasma membrane merger. It is possible that genes encoding additional proteins associated with cell-wall breakdown, plasma membrane, and trafficking can be identified in our data sets. Such proteins that are involved in trafficking and late fusion events may not have been identified by our assays for chemotropic interactions and fusion frequency; Δ*Prm-1* mutants show normal chemotropic interactions and oscillation of MAK2 and SO, but have a ~50% reduction in plasma membrane merger (Fleissner *et al.* 2009a). In our data sets, we identified a number of genes dependent on PP1 for expression that encode proteins involved in vesicle trafficking, such as a homolog to *S. cerevisiae SCN2* (NCU00566), which encodes a v-SNARE involved in the fusion of Golgi-derived secretory vesicles with the plasma membrane. Mutations in a gene encoding a homolog to calcium neuronal sensor-1 (NCU04379; *cse-1*)—which localizes to the Golgi and is involved in regulated secretion in neurons—reduce, but do not abolish, germling fusion frequency (Palma-Guerrero *et al.* 2013). Fusion frequencies are not restored when Δ*cse-1* germlings are paired with wild-type germlings. This phenotype is similar to that of Δ*ham-12* mutants, where no differences in fusion frequencies were observed between Δ*ham-12* + Δ*ham-12* germlings and Δ*ham-12* + wild-type germlings. In the future, epistasis and colocalization studies will provide additional clues for the function of these proteins during the processes of germling communication, chemotropic interactions, and cell fusion.

Acknowledgments

We thank Nick Salem for assistance with early screening of the mutants; David Kowbel for assistance with RNA-seq experiments; and Ken Allen (Yale Medical School) for kindly providing us with the PMA-1 antibody. We acknowledge use of material generated by a National Institutes of Health P01 GM068087 grant entitled "Functional Analysis of a Model Filamentous Fungus." The work in this study was funded by a National Science Foundation grant to N.L.G. (MCB 1121311).

Literature Cited

Aguilar, P. S., M. K. Baylies, A. Fleissner, L. Helming, N. Inoue *et al.*, 2013 Genetic basis of cell-cell fusion mechanisms. Trends Genet. 29: 427–437.

Aldabbous, M. S., M. G. Roca, A. Stout, I. C. Huang, N. D. Read *et al.*, 2010 The *ham-5*, *rcm-1* and *rco-1* genes regulate hyphal fusion in *Neurospora crassa*. Microbiology 156: 2621–2629.

Alspaugh, J. A., J. R. Perfect, and J. Heitman, 1998 Signal transduction pathways regulating differentiation and pathogenicity of *Cryptococcus neoformans*. Fungal Genet. Biol. 25: 1–14.

Aramayo, R., Y. Peleg, R. Addison, and R. Metzenberg, 1996 Asm-1(+), a *Neurospora crassa* gene related to transcriptional regulators of fungal development. Genetics 144: 991–1003.

Bardwell, L., 2005 A walk-through of the yeast mating pheromone response pathway. Peptides 26: 339–350.

Bayram, O., O. S. Bayram, Y. L. Ahmed, J. Maruyama, O. Valerius *et al.*, 2012 The *Aspergillus nidulans* MAPK module *AnSte11-Ste50-Ste7-Fus3* controls development and secondary metabolism. PLoS Genet. 8: e1002816.

Blackwell, E., H. J. Kim, and D. E. Stone, 2007 The pheromone-induced nuclear accumulation of the Fus3 MAPK in yeast

depends on its phosphorylation state and on Dig1 and Dig2. BMC Cell Biol. 8: 44.

Borneman, A. R., M. J. Hynes, and A. Andrianopoulos, 2001 An STE12 homolog from the asexual, dimorphic fungus *Penicillium marneffei* complements the defect in sexual development of an *Aspergillus nidulans steA* mutant. Genetics 157: 1003–1014.

Borneman, A. R., T. A. Gianoulis, Z. D. Zhang, H. Yu, J. Rozowsky *et al.*, 2007 Divergence of transcription factor binding sites across related yeast species. Science 317: 815–819.

Bowman, E. J., and B. J. Bowman, 1988 Purification of vacuolar membranes, mitochondria, and plasma membranes from *Neurospora crassa* and modes of discriminating among the different H+-ATPases. Methods Enzymol. 157: 562–573.

Bowman, S. M., A. Piwowar, M. e. Al Dabbous, J. Vierula, and S. J. Free, 2006 Mutational analysis of the glycosylphosphatidylinositol (GPI) anchor pathway demonstrates that GPI-anchored proteins are required for cell wall biogenesis and normal hyphal growth in *Neurospora crassa*. Eukaryot. Cell 5: 587–600.

Cano-Dominguez, N., K. Alvarez-Delfin, W. Hansberg, and J. Aguirre, 2008 NADPH oxidases NOX-1 and NOX-2 require the regulatory subunit NOR-1 to control cell differentiation and growth in *Neurospora crassa*. Eukaryot. Cell 7: 1352–1361.

Chang, Y. C., L. C. Wright, R. L. Tscharke, T. C. Sorrell, C. F. Wilson *et al.*, 2004 Regulatory roles for the homeodomain and C2H2 zinc finger regions of *Cryptococcus neoformans* Ste12alphap. Mol. Microbiol. 53: 1385–1396.

Chen, E. H., E. Grote, W. Mohler, and A. Vignery, 2007 Cell-cell fusion. FEBS Lett. 581: 2181–2193.

Colot, H. V., G. Park, G. E. Turner, C. Ringelberg, C. M. Crew *et al.*, 2006 A high-throughput gene knockout procedure for *Neurospora* reveals functions for multiple transcription factors. Proc. Natl. Acad. Sci. USA 103: 10352–10357.

de Hoon, M. J., S. Imoto, J. Nolan, and S. Miyano, 2004 Open source clustering software. Bioinformatics 20: 1453–1454.

Dettmann, A., J. Illgen, S. Marz, T. Schurg, A. Fleissner *et al.*, 2012 The NDR kinase scaffold HYM1/MO25 is essential for MAK2 map kinase signaling in *Neurospora crassa*. PLoS Genet. 8: e1002950.

Dunlap, J. C., K. A. Borkovich, M. R. Henn, G. E. Turner, M. S. Sachs *et al.*, 2007 Enabling a community to dissect an organism: overview of the Neurospora functional genomics project. Adv. Genet. 57: 49–96.

Elion, E. A., B. Satterberg, and J. E. Kranz, 1993 FUS3 phosphorylates multiple components of the mating signal transduction cascade: evidence for STE12 and FAR1. Mol. Biol. Cell 4: 495–510.

Ellison, C., C. Hall, D. Kowbel, J. Welch, R. Brem *et al.*, 2011 Population genomics and local adaptation in wild isolates of a model microbial eukaryote. Proc. Natl. Acad. Sci. USA 7: 2831–2836.

Errede, B., and G. Ammerer, 1989 STE12, a protein involved in cell-type-specific transcription and signal transduction is yeast, is part of protein-DNA complexes. Genes Dev. 3: 1349–1361.

Fleissner, A., S. Sarkar, D. J. Jacobson, M. G. Roca, N. D. Read *et al.*, 2005 The *so* locus is required for vegetative cell fusion and postfertilization events in *Neurospora crassa*. Eukaryot. Cell 4: 920–930.

Fleissner, A., A. R. Simonin, and N. L. Glass, 2008 Cell fusion in the filamentous fungus, *Neurospora crassa*. Methods Mol. Biol. 475: 21–38.

Fleissner, A., S. Diamond, and N. L. Glass, 2009a The *Saccharomyces cerevisiae PRM1* homolog in *Neurospora crassa* is involved in vegetative and sexual cell fusion events but also has postfertilization functions. Genetics 181: 497–510.

Fleissner, A., A. C. Leeder, M. G. Roca, N. D. Read, and N. L. Glass, 2009b Oscillatory recruitment of signaling proteins to cell tips promotes coordinated behavior during cell fusion. Proc. Natl. Acad. Sci. USA 106: 19387–19392.

Freitag, M., P. C. Hickey, N. B. Raju, E. U. Selker, and N. D. Read, 2004 GFP as a tool to analyze the organization, dynamics and function of nuclei and microtubules in *Neurospora crassa*. Fungal Genet. Biol. 41: 897–910.

Fu, C., P. Iyer, A. Herkal, J. Abdullah, A. Stout *et al.*, 2011 Identification and characterization of genes required for cell-to-cell fusion in *Neurospora crassa*. Eukaryot. Cell 10: 1100–1109.

Gancedo, J. M., 2001 Control of pseudohyphae formation in *Saccharomyces cerevisiae*. FEMS Microbiol. Rev. 25: 107–123.

Gustin, M. C., J. Albertyn, M. Alexander, and K. Davenport, 1998 MAP kinase pathways in the yeast *Saccharomyces cerevisiae*. Microbiol. Mol. Biol. Rev. 62: 1264–1300.

Heiman, M. G., and P. Walter, 2000 Prm1p, a pheromone-regulated multispanning membrane protein, facilitates plasma membrane fusion during yeast mating. J. Cell Biol. 151: 719–730.

Hou, Z., C. Xue, Y. Peng, T. Katan, H. C. Kistler *et al.*, 2002 A mitogen-activated protein kinase gene (MGV1) in *Fusarium graminearum* is required for female fertility, heterokaryon formation, and plant infection. Mol. Plant Microbe Interact. 15: 1119–1127.

Hutchison, E., S. Brown, C. Tian, and N. L. Glass, 2009 Transcriptional profiling and functional analysis of heterokaryon incompatibility in *Neurospora crassa* reveals that reactive oxygen species, but not metacaspases, are associated with programmed cell death. Microbiology 155: 3957–3970.

Jedd, G., and N. H. Chua, 2000 A new self-assembled peroxisomal vesicle required for efficient resealing of the plasma membrane. Nat. Cell Biol. 2: 226–231.

Jun, S. C., S. J. Lee, H. J. Park, J. Y. Kang, Y. E. Leem *et al.*, 2011 The MpkB MAP kinase plays a role in post-karyogamy processes as well as in hyphal anastomosis during sexual development in *Aspergillus nidulans*. J. Microbiol. 49: 418–430.

Kim, H., and K. Borkovich, 2004 A pheromone receptor gene, *pre-1,* is essential for mating type-specific directional growth and fusion of trichogynes and female fertility in *Neurospora crassa*. Mol. Microbiol. 52: 1781–1798.

Kim, H., and K. A. Borkovich, 2006 Pheromones are essential for male fertility and sufficient to direct chemotropic polarized growth of trichogynes during mating in *Neurospora crassa*. Eukaryot. Cell 5: 544–554.

Langmead, B., C. Trapnell, M. Pop, and S. L. Salzberg, 2009 Ultrafast and memory-efficient alignment of short DNA sequences to the human genome. Genome Biol. 10: R25.

Li, D., P. Bobrowicz, H. H. Wilkinson, and D. J. Ebbole, 2005 A mitogen-activated protein kinase pathway essential for mating and contributing to vegetative growth in *Neurospora crassa*. Genetics 170: 1091–1104.

Maddi, A., S. M. Bowman, and S. J. Free, 2009 Trifluoromethanesulfonic acid-based proteomic analysis of cell wall and secreted proteins of the ascomycetous fungi *Neurospora crassa* and *Candida albicans*. Fungal Genet. Biol. 46: 768–781.

Maddi, A., A. Dettman, C. Fu, S. Seiler, and S. J. Free, 2012 WSC-1 and HAM-7 are MAK-1 MAP kinase pathway sensors required for cell wall integrity and hyphal fusion in *Neurospora crassa*. PLoS ONE 7: e42374.

Madhani, H. D., and G. R. Fink, 1997 Combinatorial control required for the specificity of yeast MAPK signaling. Science 275: 1314–1317.

Maerz, S., A. Dettmann, C. Ziv, Y. Liu, O. Valerius *et al.*, 2009 Two NDR kinase-MOB complexes function as distinct modules during septum formation and tip extension in *Neurospora crassa*. Mol. Microbiol. 74: 707–723.

Margolin, B. S., M. Freitag, and E. U. Selker, 1997 Improved plasmids for gene targeting at the *his-3* locus of *Neurospora crassa* by electroporation. Fungal Genet. Newsl. 44: 34–36.

McCluskey, K., 2003 The Fungal Genetics Stock Center: from molds to molecules. Adv. Appl. Microbiol. 52: 245–262.

McNally, M. T., and S. J. Free, 1988 Isolation and characterization of a *Neurospora* glucose-repressible gene. Curr. Genet. 14: 545–551.

Meiklejohn, C. D., and J. P. Townsend, 2005 A Bayesian method for analysing spotted microarray data. Brief. Bioinform. 6: 318–330.

Nolting, N., and S. Poggeler, 2006 A STE12 homologue of the homothallic ascomycete *Sordaria macrospora* interacts with the MADS box protein MCM1 and is required for ascosporogenesis. Mol. Microbiol. 62: 853–868.

Palma-Guerrero, J., C. R. Hall, D. Kowbel, J. Welch, J. W. Taylor *et al.*, 2013 Genome wide association identifies novel loci involved in fungal communication. PLoS Genet. 9: e1003669.

Pandey, A., M. G. Roca, N. D. Read, and N. L. Glass, 2004 Role of a mitogen-activated protein kinase pathway during conidial germination and hyphal fusion in *Neurospora crassa*. Eukaryot. Cell 3: 348–358.

Pandit, A., and R. Maheshwari, 1994 A simple method of obtaining pure microconidia in *Neurospora crassa*. Fungal Genet. Newsl. 41: 64–65.

Park, G., G. Y. Xue, L. Zheng, S. Lam, and J. R. Xu, 2002 *MST12* regulates infectious growth but not appressorium formation in the rice blast fungus *Magnaporthe grisea*. Mol. Plant Microbe Interact. 15: 183–192.

Park, G., K. S. Bruno, C. J. Staiger, N. J. Talbot, and J. R. Xu, 2004 Independent genetic mechanisms mediate turgor generation and penetration peg formation during plant infection in the rice blast fungus. Mol. Microbiol. 53: 1695–1707.

Primig, M., H. Winkler, and G. Ammerer, 1991 The DNA binding and oligomerization domain of MCM1 is sufficient for its interaction with other regulatory proteins. EMBO J. 10: 4209–4218.

Read, N. D., A. Fleissner, M. G. Roca, and N. L. Glass, 2010 Hyphal fusion, pp. 260–273 in *Cellular and Molecular Biology of Filamentous Fungi*, edited by K. A. Borkovich, and D. J. Ebbole. ASM Press, Washington, DC.

Read, N. D., A. B. Goryachev, and A. Lichius, 2012 The mechanistic basis of self-fusion between conidial anastomosis tubes during fungal colony initiation. Fungal Biol. Rev. 26: 1–11.

Ren, B., F. Robert, J. J. Wyrick, O. Aparicio, E. G. Jennings *et al.*, 2000 Genome-wide location and function of DNA binding proteins. Science 290: 2306–2309.

Ren, P., D. J. Springer, M. J. Behr, W. A. Samsonoff, S. Chaturvedi *et al.*, 2006 Transcription factor STE12alpha has distinct roles in morphogenesis, virulence, and ecological fitness of the primary pathogenic yeast *Cryptococcus gattii*. Eukaryot. Cell 5: 1065–1080.

Rispail, N., and A. Di Pietro, 2010 The homeodomain transcription factor Ste12: connecting fungal MAPK signalling to plant pathogenicity. Commun. Integr. Biol. 3: 328.

Roberts, A., C. Trapnell, J. Donaghey, J. L. Rinn, and L. Pachter, 2011 Improving RNA-Seq expression estimates by correcting for fragment bias. Genome Biol. 12: R22.

Roca, G. M., N. D. Read, and A. E. Wheals, 2005a Conidial anastomosis tubes in filamentous fungi. FEMS Microbiol. Lett. 249: 191–198.

Roca, M., J. Arlt, C. Jeffree, and N. Read, 2005b Cell biology of conidial anastomosis tubes in *Neurospora crassa*. Eukaryot. Cell 4: 911–919.

Roman, E., D. M. Arana, C. Nombela, R. Alonso-Monge, and J. Pla, 2007 MAP kinase pathways as regulators of fungal virulence. Trends Microbiol. 15: 181–190.

Roper, M., A. Simonin, P. C. Hickey, A. Leeder, and N. L. Glass, 2013 Nuclear dynamics in a fungal chimera. Proc. Natl. Acad. Sci. USA 110: 12875–12880.

Ruepp, A., A. Zollner, D. Maier, K. Albermann, J. Hani *et al.*, 2004 The FunCat, a functional annotation scheme for systematic classification of proteins from whole genomes. Nucleic Acids Res. 32: 5539–5545.

Simonin, A. R., C. G. Rasmussen, M. Yang, and N. L. Glass, 2010 Genes encoding a striatin-like protein (*ham-3*) and a forkhead associated protein (*ham-4*) are required for hyphal fusion in *Neurospora crassa*. Fungal Genet. Biol. 47: 855–868.

Simonin, A., J. Palma-Guerrero, M. Fricker, and N. L. Glass, 2012 Physiological significance of network organization in fungi. Eukaryot. Cell 11: 1345–1352.

Tedford, K., S. Kim, D. Sa, K. Stevens, and M. Tyers, 1997 Regulation of the mating pheromone and invasive growth responses in yeast by two MAP kinase substrates. Curr. Biol. 7: 228–238.

Tian, C., T. Kasuga, M. S. Sachs, and N. L. Glass, 2007 Transcriptional profiling of cross pathway control in *Neurospora crassa* and comparative analysis of the Gcn4 and CPC1 regulons. Eukaryot. Cell 6: 1018–1029.

Tollot, M., J. Wong Sak Hoi, D. van Tuinen, C. Arnould, O. Chatagnier *et al.*, 2009 An STE12 gene identified in the mycorrhizal fungus *Glomus intraradices* restores infectivity of a hemibiotrophic plant pathogen. New Phytol. 181: 693–707.

Tompa, M., N. Li, T. L. Bailey, G. M. Church, B. De Moor *et al.*, 2005 Assessing computational tools for the discovery of transcription factor binding sites. Nat. Biotechnol. 23: 137–144.

Tsuji, G., S. Fujii, S. Tsuge, T. Shiraishi, and Y. Kubo, 2003 The *Colletotrichum lagenarium Ste12*-like gene *CST1* is essential for appressorium penetration. Mol. Plant Microbe Interact. 16: 315–325.

Vallim, M. A., K. Y. Miller, and B. L. Miller, 2000 *Aspergillus* SteA (sterile12-like) is a homeodomain-C2/H2-Zn+2 finger transcription factor required for sexual reproduction. Mol. Microbiol. 36: 290–301.

Vogel, H. J., 1956 A convenient growth medium for *Neurospora*. Microbiol. Genet. Bull. 13: 42–46.

Wei, H., N. Requena, and R. Fischer, 2003 The MAPKK kinase SteC regulates conidiophore morphology and is essential for heterokaryon formation and sexual development in the homothallic fungus *Aspergillus nidulans*. Mol. Microbiol. 47: 1577–1588.

Westergaard, M., and H. K. Mitchell, 1947 Neurospora V. A synthetic medium favoring sexual reproduction. Am. J. Bot. 34: 573–577.

Wong Sak Hoi, J., and B. Dumas, 2010 Ste12 and Ste12-like proteins, fungal transcription factors regulating development and pathogenicity. Eukaryot. Cell 9: 480–485.

Xiang, Q., C. Rasmussen, and N. L. Glass, 2002 The *ham-2* locus, encoding a putative transmembrane protein, is required for hyphal fusion in *Neurospora crassa*. Genetics 160: 169–180.

Yuan, Y. L., and S. Fields, 1991 Properties of the DNA-binding domain of the *Saccharomyces cerevisiae* STE12 protein. Mol. Cell. Biol. 11: 5910–5918.

Yuan, Y. O., I. L. Stroke, and S. Fields, 1993 Coupling of cell identity to signal response in yeast: interaction between the alpha 1 and STE12 proteins. Genes Dev. 7: 1584–1597.

Zeitlinger, J., I. Simon, C. T. Harbison, N. M. Hannett, T. L. Volkert *et al.*, 2003 Program-specific distribution of a transcription factor dependent on partner transcription factor and MAPK signaling. Cell 113: 395–404.

Zheng, W., H. Zhao, E. Mancera, L. M. Steinmetz, and M. Snyder, 2010 Genetic analysis of variation in transcription factor binding in yeast. Nature 464: 1187–1191.

Communicating editor: E. U. Selker

GENETICS

Supporting Information
http://www.genetics.org/lookup/suppl/doi:10.1534/genetics.113.156984/-/DC1

Early Colony Establishment in *Neurospora crassa* Requires a MAP Kinase Regulatory Network

Abigail C. Leeder, Wilfried Jonkers, Jingyi Li, and N. Louise Glass

DOI: 10.1534/genetics.113.156984

Files S1-S2

Available for download at http://www.genetics.org/lookup/suppl/doi:10.1534/genetics.113.156984/-/DC1

File S1

Supplemental Dataset 1

Sheet 1: Genes identified that are regulated by PP-1 either positively (at least 1.5-fold down in Δ*pp-1*) or negatively (at least 1.5-fold up in Δ*pp-1*) using RNAseq analysis of cells grown for five hours

Sheet 2: Functional categories present among the genes that are positively or negatively regulated by PP-1 as given in Sheet 1 (categories overrepresented, $p<0.05$, are given in bold)

File S2

Supplemental Dataset 2

Sheet 1: Genes identified that are regulated by MAK-2 either positively (down in Δmak-2q100G) or negatively (up in Δmak-2q100G) after addition of 1NM-PP1 compared to treatment with DMSO alone

Sheet 2: Functional categories present among the genes that are positively or negatively regulated by MAK-2 as given in sheet 1 (categories overrepresented, $p<0.05$, are given in bold)

Table S1 Primers Used In This Study

Primer Name	Sequence	Primer Name	Sequence
Pp-1-Paci-R06	CTTTAATTAAAAACTCTAGCTCGTTTCGCA	NCU00995R2	GCGGATAACAATTTCACACAGGAAACAGCACGACCATCGAATTCCTACC
Pp-1-Spei-F06	CGACTAAGTATGTATTCTTCGCAGCATGC	NCU01121F1	GTAACGCCAGGGTTTTCCCAGTCACGACGGAAAGACTCTCCAGATCAGC
Pp-1p-Noti-F06	GCGGCCGCGACCATAGTGGTGTAGACTACT	NCU01121R1	ATCCACTTAACGTTACTGAAATCTCCAACGGTATTGTTGGGAGTACTGG
Pp-1p-Spei-R06	CGACTAGTTCCAAGCTTAAAAACCTCCTTGATA	NCU01121F2	CTCCTTCAATATCATCTTCTGTCTCCGACCTAGGAAATACGAAGGACGG
Pp-1 Sgra1-F06	TCTACCCACCGGCGAGTATG	NCU01121R2	GCGGATAACAATTTCACACAGGAAACAGCAGTTACGACGAAACACCCAC
Pp-1-Sfii-R06	AAAGAGGACGAGTTGGCCTGCTGGTGGGCCTTG	NCU01380F1	GTAACGCCAGGGTTTTCCCAGTCACGACGATATGCGGAGGCACTTCAAG
Pp1-Smtrpr06	CGCTGTAACAGAAGAACACCTT	NCU01380R1	ATCCACTTAACGTTACTGAAATCTCCAACTTGTGCTGAGGCTATCCGTT
Pp1-Smtrp-F06	AAGGTGTTCTTCTGTTACAGCG	NCU01380F2	CTCCTTCAATATCATCTTCTGTCTCCGACACCCTGAGCTTTATGTGACC
Pp-1-Smc-F06	TACGTCAGCTCATACAGCCAGAAG	NCU01380R2	GCGGATAACAATTTCACACAGGAAACAGCAAGCTCTATTGGCATGGAGG
Pp-1-Smc-R06	CTTCTGGCTGTATGAGCTGACGTA	F00811	GCGCGCTTACTCATTGAAG
Pp-1-Afiii-F06	CGTTTGGAGCACCTTAAGAG	R00811	GATAGATGGCGCAAAGGATG
Pp-1-Nsii-R06	GTAGATTGGAAGGGTGAATG	F00995	GAGGCAAGACGGTAAGTTGG
Fqpcr00881	TGCTCACATCAACACTCC	R00995	TCCGGTTGGTATGTTGGTTT
Rqpcr00881	CCGAGGTTGACGTAGATA	F01121	CAGGGGAAAGCAATCAAGAG
Fqpcr04732	CAAGTATAACTCGGCCTG	R01121	TCGTCAATCTCCTCCTCGTT
Rqpcr04732	TAGCACCTCGTGACAATG	F01380	CCATCGTCCAACTCTTCCTC
Fqpcr02613	GCTGGTTTGATTGGGGTAGA	R01380	TTCATGAGCATGTGTGCTTG
Rqpcr02613	AAGTAGGGGCCGAGTTTGAT	F09693	GCAGTCCAGTGGTGAAGGAT
Fqpcr02246	GCTTGCCTCTCACGACTACC	R09693	CCGTTGACCCAGTAGGTTTG
Rqpcr02246	CGGAGCTAAAGCTCAAGGTG	Hygrupflk	GAATAGAGTAGATGCCGACC
Fqpcrprm1	TCTGCTCCAACAACTCCTTC	Ccg-4_F	CTTCTCCGTGACACCACCTT
Rqpcrprm1	CCGCGATATTCAATGTAGCC	Ccg-4_R	TCATCGGAGTGAGCAGTGAG
NCU09693F1	GTAACGCCAGGGTTTTCCCAGTCACGACGGTGCCTGGTTTTCTCGACTT	Mfa-1_F	CGGTATCTCGCCTCTCAACGT
NCU09693R1	ATCCACTTAACGTTACTGAAATCTCCAACTCTACGGACATAGTCGAGGT	Mfa-1_R	GGTGCTCCCATTGTGCAGA
NCU09693F2	CTCCTTCAATATCATCTTCTGTCTCCGACTTGGTCGACCACTATTTCCC	Pre-1_F	GAATGCTTTCCACGTCCCTA
NCU09693R2	GCGGATAACAATTTCACACAGGAAACAGCCGTCATAATGGAAGACGGGA	Pre-1_R	AAGGCGGTAGGATTGTTGTG
NCU00811F1	GTAACGCCAGGGTTTTCCCAGTCACGACGCAGTCTACCAAGGAACGACC	Pre-2_F	CACCAACTTTTCCTCCTCCA
NCU00811R1	ATCCACTTAACGTTACTGAAATCTCCAACCCAAGGAGTGTTGGTGTAGC	Pre-2_R	GTCGTCGTCGTGGTGTTATG
NCU00811F2	CTCCTTCAATATCATCTTCTGTCTCCGACTACGGGCTACGTTATCTAGG	04732F	AGATCTAGACATGCCCCTTGGTATCAGGA
NCU00811R2	GCGGATAACAATTTCACACAGGAAACAGCAGTGCTTTCACTACCAGACC	04732R	GGGCCCTCATTCAATTAATTAACTACCAAATCTCCTCTTCACTCC
NCU00995F1	GTAACGCCAGGGTTTTCCCAGTCACGACGTTGGTTCCTAGTACTCCTCG	Fgfp+8xgly	TTTGGATCCCGGCGGCGGTGGTGGCGGCGGTGGTATGGTGAGCAAGGGCGAG
NCU00995R1	ATCCACTTAACGTTACTGAAATCTCCAACCTAGTCCGTCACATTGAAGC	Rgfp+8xgly	AAAGGATCCCCACCGCCGCCACCACCGCCGCCCTTGTACAGCTCGTCCATGC
NCU00995F2	CTCCTTCAATATCATCTTCTGTCTCCGACGGGATGGGTTCGTTGAGATA		

Table S2 Clusters Of Genes Showing Temporal Expression During 3-8 Hr Time Germination Time Course and Genes Found Uniquely Higher Or Lower Expressed In The 4-6 Hr Loop. Genes ID Numbers In Bold Are Genes Up Regulated In The Δ*Pp-1* Mutant Compared To Wild Type.

Gene ID	Annotation	Cluster	Gene ID	Annotation	Cluster
NCU00566	Synaptobrevin	1	NCU00601	Nf	2
NCU00881	*Ham-7*	1	NCU00746	*Crp-68*	2
NCU00906	Hypothetical	1	NCU01380	Hypothetical	2
NCU01183	*Gtp-1*	1	NCU01697	Hypothetical	2
NCU01772	DNA-Directed RNA Polymerase III	1	NCU02176	Hypothetical	2
NCU02500	*Ccg-4*	1	NCU02458	Hypothetical	2
NCU02635	Mannan Polymerase Complexes MNN9 Subunit	1	NCU03196	Cyclin Pch1	2
NCU02644	Hypothetical	1	NCU03868	Hypothetical	2
NCU03276	*Bem46*	1	NCU04429	Mitochondrial Import Protein Mmp37	2
NCU03669	Adomet-Dependent Rrna Methyltransferase Spb1	1	NCU04729	Hypothetical	2
NCU03708	Hypothetical	1	NCU05178	Hypothetical	2
NCU03794	Periodic Tryptophan Protein 2	1	NCU05357	Predicted	2
NCU03830	Hypothetical	1	NCU06373	Hypothetical	2
NCU03837	Snf1 Kinase Complex Beta-Subunit Gal83	1	**NCU08457**	Eas	2
NCU03960	Hypothetical	1	NCU08833	Hypothetical	2
NCU04122	Malate Dehydrogenase	1	NCU10052	Hypothetical	2
NCU04344	Eif2b-Alpha	1	**NCU00209**	Hypothetical	3
NCU04611	Transcription Elongation Factor Spt-6	1	NCU00265	Hypothetical	3
NCU04732	*Ham-11*	1	**NCU00309**	WSC Domain-Containing Protein	3
NCU04834	*Phy-1*	1	**NCU01121**	Hypothetical	3
NCU05194	DNA Replication Licensing Factor Mcm6	1	NCU01618	Predicted	3
NCU05337	Predicted	1	**NCU04047**	Hypothetical	3
NCU05400	Hypothetical	1	NCU04349	*Stk-58 (CHECK)*	3
NCU05814	Hypothetical	1	**NCU04452**	*Mig-3*	3
NCU06115	Hypothetical	1	NCU05127	D-Alanyl-Alanine Synthetase A	3
NCU06919	Hypothetical	1	NCU05495	*Ccg-16*	3
NCU07029	Hypothetical	1	NCU05502	Hypothetical	3
NCU07313	Chromosome Transmission Fidelity Protein 18	1	NCU05831	Hypothetical	3
NCU07503	Hypothetical	1	NCU06514	Hypothetical	3
NCU07528	Trna Pseudouridine Synthase	1	NCU07439	Hypothetical	3
NCU07609	MFS Transporter	1	NCU07802	Hypothetical	3
NCU07610	Taurine Dioxygenase	1	NCU09562	Hypothetical	3
NCU07719	Isopentenyl-Diphosphate Delta-Isomerase	1	NCU09693	Hypothetical	3
NCU08332	*Hex-1*	1	NCU09802	Hypothetical	3
NCU08656	Hypothetical	1	**NCU09894**	CCAAT-Box-Binding Transcription Factor	3
NCU08824	Molybdopterin Binding Domain-Containing Protein	1	NCU00811	Hypothetical	4

NCU09427	*Gpr-3*	1	NCU00995	Hypothetical	4
NCU09498	Hypothetical	1	**NCU02361**	Formamidase	4
NCU09560	Superoxide Dismutase	1	**NCU02727**	Glycine Cleavage System T Protein	4
NCU10292	Porphobilinogen Deaminase	1	**NCU06360**	Histidinol-Phosphate Aminotransferase	4

Genes Uniquely Down Regulated In The 4-6 Hour Loop		Genes Uniquely Up Regulated In The 4-6 Hour Loop	
Gene ID	Annotation	Gene ID	Annotation
1nc380_040	Hypothetical	**NCU00973**	Hypothetical
NCU00354	Hypothetical	**NCU01124**	Hypothetical
NCU00556	RNA Binding Protein	**NCU02729**	Transducin Family Protein
NCU01189	Hypothetical	**NCU03153**	Hypothetical
NCU01191	Hypothetical	**NCU03192**	Hypothetical
NCU01459	Tan Spore *Asl-2*	**NCU04966**	Predicted Protein
NCU01545	*Atg-8*	**NCU09300**	RNA Polymerase II CTD Phosphatase Fcp1
NCU02298	Hypothetical	**NCU09992**	Serine Peptidase
NCU02465	Hypothetical		
NCU02488	Hypothetical		
NCU03013	Anchored Cell Wall Protein-10, *Acw-10*		
NCU03344	Hypothetical		
NCU04192	Vacuolar Aspartyl Aminopeptidase *Lap4*		
NCU04278	Hypothetical		
NCU04542	Hypothetical		
NCU05233	P60 Domain-Containing Protein		
NCU05395	Hypothetical		
NCU05408	Predicted Protein		
NCU05593	Topogenesis Of Mitochondrial Outer Membrane Beta Barrel Proteins 55, *Tob-55*		
NCU05856	Hypothetical		
NCU05959	Vesicle Transport V-SNARE Protein VTI1		
NCU06698	Glycogenin *Gnn*		
NCU07091	Hypothetical		
NCU07817	Non-Anchored Cell Wall Protein-3, *Ncw-3*		
NCU08037	Hypothetical		
NCU08257	Hypothetical		

Table S3 (A) functional categories overrepresented (P<0.05) present among the genes identified that are positively regulated by pp-1 (down in Δpp-1) in at least one time point during the three to eight or the four to six hour time course. (B) functional categories overrepresented (P<0.05) present among the genes identified that are negatively regulated by pp-1 (up in Δ*pp-1*) in at least one time point during the three to eight or the four to six hour time course.

A.

Functional category	Abs Set	Rel Set	Genes Set	Abs Genome	Rel Genome	Rel Set/Rel Genome	P-Value
14.13.04 Lysosomal and vacuolar protein degradation	2	2.85	NCU01545 NCU04192	13	0.12	23.75	0.004
30.05.02.24 G-protein coupled receptor signalling pathway	2	2.85	NCU01545 NCU09427	17	0.16	17.812	0.006
30.05.02.24.04 Gamma-aminobutyric acid signalling pathway	1	1.42	NCU01545	1	0	0	0.007
30.05 transmembrane signal transduction	3	4.28	NCU01545 NCU09427 NCU04834	63	0.62	6.90	0.009
99 Unclassified proteins	50	71.4	NCU05178 NCU05395 NCU00746 NCU05593 NCU01697 NCU06373 NCU05856 NCU00354 NCU03708 NCU07817 NCU03344 NCU05814 NCU02176 NCU05495 NCU00881 NCU02298 NCU21668 NCU04122 NCU06115 NCU07802 NCU04278 NCU07439 NCU21253 NCU01189 NCU05408 NCU06919 NCU02465 NCU04542 NCU08257 NCU08037 NCU00995 NCU01191 NCU08833 NCU10052 NCU06514 NCU02488 NCU05502 NCU09562 NCU00265 NCU03960 NCU05831 NCU04429 NCU04732 NCU01380 NCU02432 NCU00811 NCU07091 NCU09693 NCU21678 NCU09802	5853	58.1	1.23	0.015
30.05.02 Non-enzymatic receptor mediated signalling	2	2.85	NCU09427 NCU01545	27	0.26	10.96153846	0.014957492
14.07.11.01 Autoproteolytic processing	1	1.42	NCU01545	7	0.06	23.66666667	0.047688778
14.13.04.02 Vacuolar protein degradation	1	1.42	NCU04192	7	0.06	23.66666667	0.047688778
16.01.01 Receptor binding	1	1.42	NCU01545	7	0.06	23.66666667	0.047688778

B.

Functional category	Abs Set	Rel Set	Genes Set	Abs Genome	Rel Genome	Rel Set/Rel Genome	P-Value
11 Transcription	8	20.5	NCU04611 NCU02729 NCU03794 NCU05194 NCU07528 NCU01772 NCU03669 NCU01183	725	7.2	2.85	0.006
11.06 rna modification	2	5.12	NCU03669 NCU07528	42	0.41	12.49	0.011
01.06.06.13 Tetraterpenes (carotinoids) metabolism	1	2.56	NCU07719	3	0.02	128.00	0.012
11.02 RNA synthesis	6	15.3	NCU01772 NCU02729 NCU04611 NCU01183 NCU03669 NCU05194	533	5.29	2.89	0.016
01.01.09.05.01 Biosynthesis of tyrosine	1	2.56	NCU06360	5	0.04	64.00	0.019
32.07.07.07 Superoxide metabolism	1	2.56	NCU09560	5	0.04	64.00	0.019
11.02.03 mRNA Synthesis	5	12.8	NCU05194 NCU01772 NCU04611 NCU02729 NCU03669	465	4.61	2.78	0.032
01.01.09.01.02 Degradation of glycine	1	2.56	NCU02727	10	0.09	28.44	0.038
01.05.05.07 C-1 compound catabolism	1	2.56	NCU02727	10	0.09	28.44	0.038
11.06.01 rRNA modification	1	2.56	NCU03669	10	0.09	28.44	0.038
11.02.03.01 General transcription activities	2	5.12	NCU04611 NCU01772	84	0.83	6.17	0.042
11.02.03.04 Transcriptional control	4	10.2	NCU02729 NCU05194 NCU04611 NCU03669	350	3.47	2.94	0.045
01.05.05 C-1 compound metabolism	1	2.56	NCU02727	12	0.11	23.27	0.046
34.11.11 Rhythm (e.g. circadian, ultradian)	1	2.56	NCU02500	12	0.11	23.27	0.046
01.01.09.01.01 Biosynthesis of glycine	1	2.56	NCU02727	13	0.12	21.33	0.049
10.01.03.03 ORI recognition and priming complex formation	1	2.56	NCU05194	13	0.12	21.33	0.049
40.01.05 Growth regulators / regulation of cell size	1	2.56	NCU02729	13	0.12	21.33	0.049

Table S4 Overlapping Gene Sets That Showed Decreased (Dn) Or Increased (Up) Expression Levels In Δ*Pp-1* And *Mak-2*^{Q100G} Datasets

Dn Δ*Pp-1* Microarray And Rnaseq	Annotation	Dn Δ*Pp-1* Rnaseq And *Mak-2* ^{Q100G} Microarray	Annotation	Dn Δ*Pp-1* Microarray And *Mak-2* ^{Q100G} Microarray	Annotation
NCU00811	Hypothetical	**NCU00881**	*Ham-7*	**NCU00881**	*Ham-7*
NCU00881	*Ham-7*	**NCU00995**	Hypothetical	**NCU00995**	Hypothetical
NCU00995	Hypothetical	NCU01328	Transketolase	**NCU01697**	Hypothetical
NCU01380	Hypothetical	NCU01509	Hypothetical	**NCU03960**	*Ham-12*
NCU01697	Hypothetical	**NCU01697**	Hypothetical	**NCU04122**	Malate Dehydrogenase
NCU03013	*Acw-10*	NCU02110	*Nox-1*	**NCU04732**	*Ham-11*
NCU03960	*Ham-12*	NCU02209	Fatty Acid Desaturase	NCU07439	Hypothetical
NCU04122	Malate Dehydrogenase	NCU02767	*Ham-6*	**NCU09693**	Hypothetical
NCU04192	Vacuolar Aspartyl Aminopeptidase	NCU03132	Hypothetical		
NCU04732	*Ham-11*	NCU03192	Hypothetical		
NCU05814	Hypothetical	NCU03396	*Nop-58*		
NCU06698	Glycogenin	**NCU03960**	*Ham-12*		
NCU07802	Hypothetical	**NCU04122**	Malate Dehyrogenase		
NCU08332	*Hex-1*	NCU04527	Hypothetical		
NCU09562	Hypothetical	NCU04647	Actin-Binding Protein		
NCU09693	Hypothetical	**NCU04732**	*Ham-11*		
		NCU05789	Secreted Glucosidase		
		NCU05835	Hypothetical		
		NCU06034	Hypothetical		
		NCU06117	Hypothetical		
		NCU06989	Hypothetical		
		NCU07192	Hypothetical		
		NCU07392	*Adv-1*		
		NCU07850	*Nor-1*		
		NCU09108	Hypothetical		
		NCU09307	*Lfd-1*		
		NCU09337	*Prm-1*		
		NCU09693	Hypothetical		

Up Δ*Pp-1* Microarray And Rnaseq	Annotation	Up Δ*Pp-1* Rnaseq And *Mak-2*^{Q100G} Microarray		Up Δ*Pp-1* Microarray And *Mak-2*^{Q100G} Microarray	
NCU00309	WSC Domain-Containing Protein	NCU03152	DUF1348 Domain-Containing Protein	NCU02727	Glycine Cleavage System T Protein
NCU02361	Formamidase	NCU03222	Hypothetical	NCU06360	Histidinol-Phosphate Aminotransferase
NCU02500	*Ccg-4*	NCU04479	Lap2		
NCU07503	Hypothetical	NCU05686	Cell Wall Glucanase		
NCU08824	Molybdopterin	NCU07953	*Aod-1*		

NCU09560	Binding Domain-Containing Protein Superoxide Dismutase	NCU09116	Aromatic Aminotransferase Aro8
		NCU09141	*Mig-9*